Scaling of nonperturbatively $O(a)$-improved Wilson fermions: Hadron spectrum, quark masses, and decay constants

M. Göckeler,[1] R. Horsley,[2] H. Perlt,[3] P. Rakow,[4] G. Schierholz,[4,5] A. Schiller,[3] and P. Stephenson[4]

[1]*Institut für Theoretische Physik, Universität Regensburg, D-93040 Regensburg, Germany*
[2]*Institut für Physik, Humboldt-Universität, D-10115 Berlin, Germany*
[3]*Institut für Theoretische Physik, Universität Leipzig, D-04109 Leipzig, Germany*
[4]*Deutsches Elektronen-Synchrotron DESY, Institut für Hochenergiephysik und HLRZ, D-15735 Zeuthen, Germany*
[5]*Deutsches Elektronen-Synchrotron DESY, D-22603 Hamburg, Germany*

We compute the hadron mass spectrum, the quark masses, and the meson decay constants in quenched lattice QCD with nonperturbatively $O(a)$-improved Wilson fermions. The calculations are done for two values of the coupling constant $\beta = 6.0$ and 6.2, and the results are compared with the predictions of ordinary Wilson fermions. We find that the improved action reduces lattice artifacts as expected. [S0556-2821(98)05609-4]

I. INTRODUCTION

The calculation of hadron masses in lattice gauge theory has a long history. Over the years there has been a steady improvement in computing power and methods allowing simulations on larger volumes and smaller quark masses with higher statistics. However, the progress to smaller lattice spacing a has been slower because of the high computer cost which increases by at least a factor of $(1/a)^5$. Since it is so expensive to reduce cutoff effects by reducing a, we should consider reducing them by improving the action.

A systematic improvement program reducing the cutoff errors order by order in a has been proposed by Symanzik [1] and developed for on-shell quantities in Ref. [2]. The standard gluonic action has discretization errors of $O(a^2)$, but those for Wilson fermions are of $O(a)$. Therefore it is the fermionic action which is most in need of improvement.

Sheikholeslami and Wohlert [3] proposed the action (we assume $r=1$ throughout the paper)

$$S_F = S_F^{(0)} - \frac{i}{2}\,\kappa g\, c_{\text{SW}}(g) a a^4 \sum_x\ \bar{\psi}(x) \sigma_{\mu\nu} F_{\mu\nu}(x) \psi(x),$$
(1)

where $S_F^{(0)}$ is the original Wilson action and

$$F_{\mu\nu}(x) = \frac{1}{8iga^2} \sum_{\mu,\nu=\pm} [U(x)_{\mu\nu} - U(x)_{\mu\nu}^\dagger].$$
(2)

In Eq. (2) the sum extends over the four plaquettes in the $\mu\nu$ plane which have x as one corner, and the plaquette operators $U(x)_{\mu\nu}$ are the products of the four link matrices comprising the plaquettes taken in a clockwise sense. If c_{SW} is appropriately chosen, this action removes all $O(a)$ errors from on-shell quantities such as the hadron masses. A nonperturbative evaluation of this function leads to [4]

$$c_{\text{SW}}(g) = \frac{1 - 0.656 g^2 - 0.152 g^4 - 0.054 g^6}{1 - 0.922 g^2}, \quad g^2 \lesssim 1. \quad (3)$$

When we talk about improved fermions in the following, we always understand that c_{SW} has been chosen according to Eq. (3).

In this paper we shall present results for the light hadron mass spectrum, the light and strange quark masses, and the light meson decay constants using the improved action. The calculation is done for two values of the coupling $\beta = 6.0$ and 6.2 which allows us to test for scaling.

The mass calculations extend our earlier work [5] where we have examined the c_{SW} dependence at $\beta = 6.0$. To exhibit the effect of improvement, we have also done calculations with Wilson fermions on the same lattices. Most of our Wilson data come from our structure function calculations [6,7], and we combine this with masses from the literature at other β values to see the dependence on a clearly.

From the meson correlation functions we also extract meson decay constants and quark masses. However, simply improving the action is not sufficient to remove all $O(a)$ errors from these quantities. Here we also have to improve the operators which is done by adding higher-dimensional terms with the same quantum numbers in an appropriate fashion.

This paper is organized as follows. In Sec. II we briefly describe our numerical method. The hadron masses are given in Sec. III, concentrating in particular on the extrapolation to the chiral limit and the scaling behavior of improved and Wilson action results. In Sec. IV we compute the light and strange quark masses using two different methods, from the axial vector current Ward identity and from the lattice bare quark masses. The meson decay constants are discussed in Sec. V. Finally, in Sec. VI we give our conclusions.

II. COMPUTATIONAL DETAILS

Our calculations have mainly been done at $\beta = 6.0$ and 6.2 on $16^3 32$, $24^3 32$, and $24^3 48$ lattices. We use Quadrics (formerly called APE) parallel computers. For the improved case the parameter c_{SW} is given from Eq. (3) as $c_{\text{SW}} = 1.769$ at $\beta = 6.0$ and $c_{\text{SW}} = 1.614$ at $\beta = 6.2$. The simulations are done for at least five different κ values in each case. This helps with the extrapolation to the chiral limit.

For the gauge field update we use a combination of 16

TABLE I. Hadron masses at $\beta=5.7$ for Sheikholeslami-Wohlert fermions with $c_{SW}=1$ and 2.25. In the bottom row we give κ_c and the mass values extrapolated to the chiral limit. The numbers in roman (italic) are from three-parameter (two-parameter) fits. The errors are bootstrap errors.

			$\beta=5.7$ $c_{SW}=1.0$				
V	κ	am_π	am_ρ	am_N	am_{a_0}	am_{a_1}	am_{b_1}
	0.1500	0.5028(17)	0.757(7)	1.135(18)	1.36(10)	1.61(19)	1.06(16)
$16^3 32$	0.1510	0.414(2)	0.711(8)	1.040(17)	1.11(17)	1.31(12)	1.11(17)
	0.1520	0.288(5)	0.660(19)	0.92(3)		1.09(17)	1.25(20)
C.L.	0.15280(14)	0	*0.605(24)*	*0.797(49)*		*0.70(36)*	*1.31(30)*
			$c_{SW}=2.25$				
V	κ	am_π	am_ρ	am_N	am_{a_0}	am_{a_1}	am_{b_1}
	0.1270	0.841(3)	1.087(8)	1.588(12)	1.64(10)	1.56(7)	1.48(13)
	0.1275	0.791(4)	1.053(10)	1.518(23)	1.56(7)	1.51(5)	1.53(9)
$16^3 32$	0.1280	0.736(3)	1.022(11)	1.453(18)	1.50(7)	1.46(4)	1.42(7)
	0.1285	0.672(5)	0.988(9)	1.399(24)	1.57(14)	1.41(6)	1.39(7)
	0.1290	0.607(7)	0.955(8)	1.320(20)	1.59(14)	1.34(8)	1.33(11)
	0.1295	0.519(11)	0.922(16)	1.23(3)	-	1.28(10)	1.33(16)
C.L.	0.13074(29)	0	*0.793(19)*	*0.948(46)*	*1.43(33)*	*1.06(16)*	*1.13(25)*

overrelaxation sweeps followed by a three-hit Metropolis update. This procedure is repeated 50 times to generate a new configuration.

The improvement term in Eq. (1) appears in the site-diagonal part of the action. The major overhead in our case is multiplication by this term during inversion of the fermion mass matrix. In our basis of Hermitian γ matrices we can rewrite this term as [8]

$$1-\frac{i}{2}\kappa g c_{SW}\sigma\cdot F = \begin{pmatrix} A & B \\ B & A \end{pmatrix}$$
$$= \frac{1}{2}\begin{pmatrix} 1 & -1 \\ 1 & 1 \end{pmatrix}\begin{pmatrix} A+B & 0 \\ 0 & A-B \end{pmatrix}$$
$$\times \begin{pmatrix} 1 & 1 \\ -1 & 1 \end{pmatrix}, \tag{4}$$

where A, B are 6×6 matrices (two-spinors with color), so that instead of a 12×12 multiplication we have two 6×6 multiplications and two inexpensive coordinate transformations. This reduces the overhead for the improvement in the inverter from 45 to 30%. Also, the inverse of the matrix in Eq. (4) is required on half the lattice due to the even-odd preconditioning. We now have to invert two 6×6 instead of a 12×12 matrix. However, this is only required once for each propagator inversion.

For the matrix inversion we mainly used the minimal residue algorithm, except for the lightest quark mass on the larger lattices where we used the BICGSTAB algorithm [9,10]. As convergence criterion we chose

$$|r|\leqslant 10^{-6} \tag{5}$$

for the residue, which is the best that can be achieved for our single precision machine.

For the mass calculations we used Jacobi smearing for source and sink. For a detailed description of our application of this procedure see Ref. [11]. We have two parameters we can use to set the size of our source, the number of smearing steps N_s and the smearing hopping parameter κ_s. We chose $N_s=50$ for $\beta=6.0$ and 100 for $\beta=6.2$ and $\kappa_s=0.21$ at both β values. This gives roughly the same rms radius in physical units in both cases, namely 0.4 fm. To define the matrix elements for the decay constants and quark masses, we have also computed correlation functions with smeared source and local sink. This does not require any additional matrix inversions.

At $\beta=6.0$ and $c_{SW}=0$ we had generated $O(5000)$ configurations for our structure function project on which we have computed the hadron masses. To these we added $O(150)$ new configurations on which we computed the meson decay constants and the chiral Ward identity. For $c_{SW}=1.769$ we have analyzed $O(1000)$ configurations. For the heavier quark masses, $\kappa=0.1487$ and $\kappa=0.1300, 0.1310, 0.1320$, respectively, the number of configurations was $O(200)$. On the 24^3 lattice we have generated $O(100)$ and $O(200)$ configurations at $c_{SW}=0$ and 1.769, respectively. At $\beta=6.2$ we only ran on 24^3 lattices. Here we have analyzed $O(100)$ configurations for $c_{SW}=0$ and $O(300)$ configurations for $c_{SW}=1.614$. We employed both relativistic and nonrelativistic wave functions [6,7], except for the high statistics runs where we only looked at the nonrelativistic wave function in order to save computer time.

Besides our calculations at $\beta=6.0$ and 6.2 we also made exploratory studies at $\beta=5.7$ to see what effect varying c_{SW} has on coarser lattices. If one decreases β, increases c_{SW} or increases κ, one starts to get problems with exceptional configurations. This showed up in nonconvergence of our fermion matrix inversions. It was, however, only a real problem at $\beta=5.7$, $c_{SW}=2.25$ and [5] $\beta=6.0$, $c_{SW}=3.0$.

TABLE II. Hadron masses at $\beta=6.0$ for Wilson fermions ($c_{SW}=0$) and improved fermions ($c_{SW}=1.769$). Otherwise the notation is the same as in Table I.

				$\beta=6.0$ $c_{SW}=0$			
V	κ	am_π	am_ρ	am_N	am_{a_0}	am_{a_1}	am_{b_1}
$16^3 32$	0.1487	0.6384(18)	0.683(2)	1.071(7)	0.885(19)	0.933(13)	0.940(19)
	0.1515	0.5037(8)	0.5696(10)	0.9019(17)	0.817(7)	0.851(7)	0.849(13)
	0.1530	0.4237(8)	0.5080(11)	0.7977(20)	0.763(11)	0.797(6)	0.809(7)
	0.1550	0.3009(10)	0.4264(14)	0.6517(30)	0.735(15)	0.717(12)	0.736(9)
$24^3 32$	0.1550	0.292(2)	0.418(5)	0.638(8)	0.610(48)	0.657(33)	0.659(35)
	0.1558	0.229(2)	0.384(7)	0.555(12)	0.616(90)	0.613(41)	0.638(38)
	0.1563	0.179(3)	0.358(11)	0.488(22)	0.88(15)	0.584(52)	0.615(44)
C.L.	0.15713(3)	0	0.327(6)	0.412(16)	*0.658(19)*	*0.632(14)*	*0.650(13)*
				$c_{SW}=1.769$			
V	κ	am_π	am_ρ	am_N	am_{a_0}	am_{a_1}	am_{b_1}
$16^3 32$	0.1300	0.707(2)	0.783(6)	1.190(6)			
	0.1310	0.627(2)	0.714(3)	1.079(7)			
	0.1320	0.545(5)	0.644(8)	0.974(16)			
	0.1324	0.5039(7)	0.6157(16)	0.932(4)	0.779(14)	0.829(12)	0.853(7)
	0.1333	0.4122(8)	0.5502(23)	0.821(5)	0.738(15)	0.773(7)	0.799(10)
	0.1342	0.2988(17)	0.487(3)	0.705(9)	0.92(5)	0.68(2)	0.775(15)
$24^3 32$	0.1342	0.3020(11)	0.491(3)	0.686(7)	0.82(3)	0.715(19)	0.758(16)
	0.1346	0.2388(14)	0.467(6)	0.626(10)	1.00(8)	0.684(26)	0.745(20)
	0.1348	0.194(4)	0.448(13)	0.593(19)	1.52(20)	0.664(34)	0.736(29)
C.L.	0.13531(1)	0	0.417(7)	0.511(15)	*0.816(33)*	*0.625(19)*	*0.710(14)*

III. HADRON MASSES

We consider hadrons where all the quarks have degenerate masses. We looked at π, ρ, nucleon (N), a_0, a_1, and b_1 masses, and we have used this nomenclature for all quark masses, not just in the chiral limit.

In our mass calculations we have made single exponential fits to meson and baryon correlators over appropriate fit ranges. The errors are determined using the bootstrap method with 50 data samples. We present our hadron mass results in Tables I, II, and III. Table II updates the results presented in

TABLE III. Hadron masses at $\beta=6.2$ for Wilson fermions ($c_{SW}=0$) and improved fermions ($c_{SW}=1.614$). Otherwise the notation is the same as in Table I.

				$\beta=6.2$ $c_{SW}=0$			
V	κ	am_π	am_ρ	am_N	am_{a_0}	am_{a_1}	am_{b_1}
$24^3 48$	0.1468	0.5258(12)	0.5585(16)	0.872(5)	0.685(8)	0.700(21)	0.695(21)
	0.1489	0.4148(13)	0.4615(19)	0.720(6)	0.589(8)	0.624(9)	0.626(9)
	0.1509	0.2947(14)	0.3672(27)	0.560(10)	0.507(14)	0.536(13)	0.540(13)
	0.1518	0.2299(15)	0.326(4)	0.487(12)	0.474(20)	0.509(16)	0.519(17)
	0.1523	0.1867(17)	0.307(6)	0.448(14)	0.479(30)	0.492(17)	0.511(21)
C.L.	0.15336(4)	0	0.255(9)	0.342(28)	*0.407(17)*	*0.449(15)*	*0.464(16)*
				$c_{SW}=1.614$			
V	κ	am_π	am_ρ	am_N	am_{a_0}	am_{a_1}	am_{b_1}
$24^3 48$	0.1321	0.5179(7)	0.5738(11)	0.877(4)	0.691(5)	0.723(6)	0.727(6)
	0.1333	0.4143(8)	0.4850(15)	0.735(5)	0.603(10)	0.642(5)	0.638(8)
	0.1344	0.3046(9)	0.4005(26)	0.592(9)	0.532(21)	0.563(7)	0.566(9)
	0.1349	0.2444(9)	0.3626(43)	0.521(13)	0.543(22)	0.529(10)	0.539(12)
	0.1352	0.2016(11)	0.3430(53)	0.485(6)	0.646(53)	0.514(13)	0.523(25)
C.L.	0.13589(2)	0	0.287(9)	0.378(18)	*0.460(21)*	*0.460(9)*	*0.465(12)*

TABLE IV. The critical values of κ, κ_c, of our data for the linear [Eq. (6)], chiral [Eq. (7)], and phenomenological fit [Eq. (8)] for the various c_{SW} parameters.

		Eq. (6)		Eq. (7)		Eq. (8)	
β	c_{SW}	κ_c	χ^2/dof	κ_c	χ^2/dof	κ_c	χ^2/dof
5.7	1.0	0.15305(5)	3.0	0.15274(15)		0.15280(14)	
	2.25	0.13120(7)	0.7	0.13065(28)	0.1	0.13074(29)	0.1
6.0	0	0.15695(1)	17.5	0.15726(5)	8.6	0.15713(3)	6.6
	1.769	0.13521(1)	11.5	0.13537(2)	1.5	0.13531(1)	1.0
6.2	0	0.15308(1)	30.8	0.15361(8)	0.7	0.15336(4)	0.0
	1.614	0.13574(1)	39.6	0.13601(3)	1.2	0.13589(2)	0.1

Ref. [5]. For the meson masses we found very little difference between using relativistic and nonrelativistic wave functions, and we settled for relativistic wave functions (except for the high statistics runs). For the nucleon we have chosen nonrelativistic wave functions [6] which performed slightly better because the effective mass plateaus extended to larger times. At $\beta=6.0$ we repeated the lightest quark mass on $16^3 32$ on the $24^3 32$ lattice, for both improved and Wilson fermions. The values agree within less than 3%. This indicates that all our results on the $16^3 32$ lattice do not suffer from significant finite size effects.

Chiral Behavior. To obtain the critical value of κ, κ_c, and the hadron masses in the chiral limit, we extrapolate our data to zero π mass. We first tried

$$m_\pi^2 = b\left(\frac{1}{\kappa} - \frac{1}{\kappa_c}\right). \qquad (6)$$

Using this relation gives a rather poor fit of the data, and we saw that there was a slight curvature in a plot of m_π^2 against $1/\kappa$. Quenched chiral perturbation theory predicts [12]
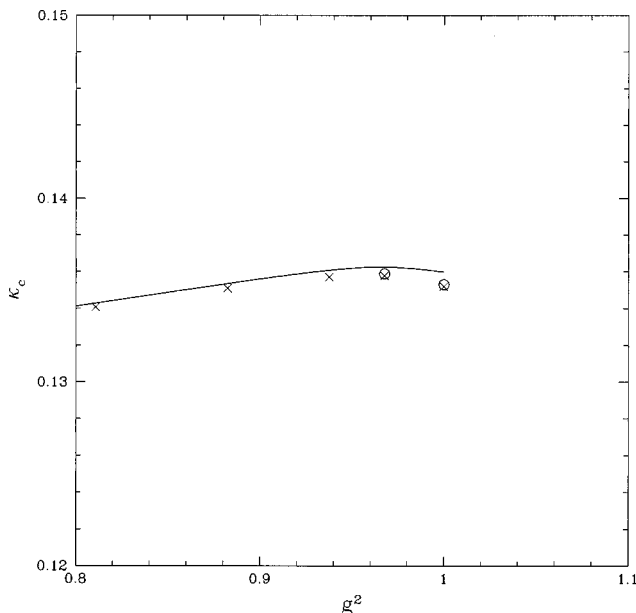
$$m_\pi^2 = b'\left(\frac{1}{\kappa} - \frac{1}{\kappa_c}\right)^{1/(1+\delta)}, \qquad (7)$$

where δ is small and positive. We made fits using this formula but found that δ was always negative. As in our previous work [5] we conclude that our κ values are too far from κ_c for the formula to be applicable. This is in agreement with observations made by other authors [13]. As an alternative parametrization of the curvature we used the phenomenological fit

$$\frac{1}{\kappa} = \frac{1}{\kappa_c} + b_2 m_\pi^2 + b_3 m_\pi^3. \qquad (8)$$

In Table IV we give the values of κ_c for the different fits. The linear fits give χ^2/dof values of up to 40. The other two fits both give acceptable values of χ^2, but Eq. (8) usually gives a lower χ^2 than Eq. (7). In the following we shall take κ_c from the phenomenological fits.
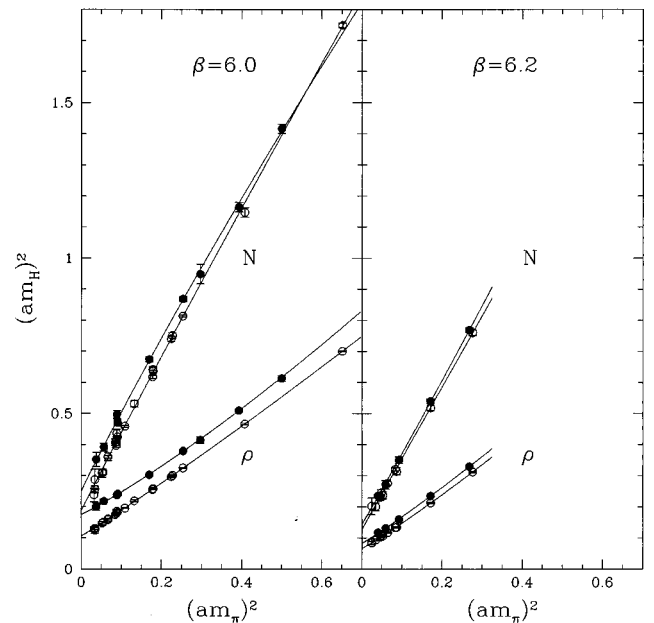

FIG. 1. The critical values of κ for improved Wilson fermions as a function of g^2 from this work ($\bigcirc$) and Ref. [4] ($\times$). The curve is the tadpole-improved result given in Eq. (10).

FIG. 2. Fits and chiral extrapolations of ρ and nucleon masses for improved ($\bullet$) and Wilson fermions ($\bigcirc$).

TABLE V. World Wilson fermion masses above $\beta = 6.0$.

β	κ	am_π	am_ρ	am_N	Lattice	Ref.
6.30	0.1400	0.789(4)	0.804(4)		$32^3 \times 48$	[16]
6.30	0.1430	0.646(6)	0.670(5)		$32^3 \times 48$	[16]
6.30	0.1460	0.4879(12)	0.5188(18)	0.8252(42)	$24^3 \times 32$	[17]
6.30	0.1480	0.382(4)	0.429(4)		$32^3 \times 48$	[16]
6.30	0.1485	0.3480(14)	0.3990(23)	0.6340(47)	$24^3 \times 32$	[17]
6.30	0.1498	0.2631(19)	0.3354(30)	0.5215(67)	$24^3 \times 32$	[17]
6.30	0.1500	0.253(6)	0.333(4)		$32^3 \times 48$	[16]
6.30	0.1505	0.2093(26)	0.3012(40)	0.4506(89)	$24^3 \times 32$	[17]
6.20	0.1468	0.5258(12)	0.5585(16)	0.872(5)	$24^3 \times 48$	this work
6.20	0.1489	0.4148(13)	0.4615(19)	0.720(6)	$24^3 \times 48$	this work
6.20	0.1509	0.2947(14)	0.3672(27)	0.560(10)	$24^3 \times 48$	this work
6.20	0.1510	0.289(1)	0.366(2)	0.566(4)	$24^3 \times 64$	[18]
6.20	0.1515	0.254(1)	0.343(3)	0.525(6)	$24^3 \times 64$	[18]
6.20	0.1518	0.2299(15)	0.326(4)	0.487(12)	$24^3 \times 48$	this work
6.20	0.1520	0.220(7)	0.327(9)	0.495(10)	$24^3 \times 48$	[19]
6.20	0.1520	0.215(1)	0.321(5)	0.48(1)	$24^3 \times 64$	[18]
6.20	0.1523	0.1867(17)	0.307(6)	0.448(14)	$24^3 \times 48$	this work
6.20	0.1526	0.158(1)	0.29(1)	0.45(3)	$24^3 \times 64$	[18]
6.17	0.1500	0.3866(12)	0.4458(18)	0.6966(40)	$32^2 \times 30 \times 40$	[20]
6.17	0.1519	0.2631(12)	0.3572(26)	0.5460(52)	$32^2 \times 30 \times 40$	[20]
6.17	0.1526	0.2064(15)	0.3245(39)	0.4848(68)	$32^2 \times 30 \times 40$	[20]
6.17	0.1532	0.1455(20)	0.2965(88)	0.4097(78)	$32^2 \times 30 \times 40$	[20]

In Fig. 1 we plot κ_c for improved Wilson fermions. We compare our results with the results of Ref. [4]. The agreement is excellent. In one-loop perturbation theory κ_c is given by [5]

$$\kappa_c = \frac{1}{8}[1 + g^2(0.108571 - 0.028989 c_{\text{SW}} - 0.012064 c_{\text{SW}}^2)].$$

(9)

TABLE VI. World Wilson fermion masses at $\beta = 6.0$.

β	κ	am_π	am_ρ	am_N	Lattice	Ref.
6.0	0.1450	0.8069(7)	0.8370(9)	1.3225(28)	$24^3 \times 54$	[21]
6.0	0.1487	0.6384(18)	0.683(2)	1.071(7)	$16^3 \times 32$	this work
6.0	0.1515	0.5037(8)	0.5696(10)	0.9019(17)	$16^3 \times 32$	this work
6.0	0.1520	0.4772(9)	0.5486(15)	0.8669(49)	$24^3 \times 54$	[21]
6.0	0.1520	0.474(1)	0.545(2)	0.861(5)	$18^3 \times 32$	[17]
6.0	0.1530	0.423(1)	0.508(3)	0.801(6)	$18^3 \times 64$	[18]
6.0	0.1530	0.4237(8)	0.5080(11)	0.7977(20)	$16^3 \times 32$	this work
6.0	0.1530	0.422(1)	0.505(1)	0.786(3)	$32^3 \times 64$	[22]
6.0	0.1540	0.364(1)	0.468(4)	0.729(7)	$18^3 \times 64$	[18]
6.0	0.1545	0.33076(28)	0.4425(10)	0.6777(21)	$24^3 \times 64$	[23]
6.0	0.1550	0.298(1)	0.431(6)	0.66(1)	$18^3 \times 64$	[18]
6.0	0.1550	0.3009(10)	0.4264(14)	0.6517(30)	$16^3 \times 32$	this work
6.0	0.1550	0.29642(27)	0.4220(12)	0.6393(27)	$24^3 \times 64$	[23]
6.0	0.1550	0.292(2)	0.418(5)	0.638(8)	$24^3 \times 32$	this work
6.0	0.1550	0.2967(15)	0.4218(42)	0.6440(85)	$24^3 \times 54$	[21]
6.0	0.1550	0.296(1)	0.422(2)	0.630(5)	$32^3 \times 64$	[22]
6.0	0.1555	0.25864(33)	0.4016(17)	0.6003(37)	$24^3 \times 64$	[23]
6.0	0.1555	0.2588(16)	0.3982(61)	0.6007(109)	$24^3 \times 54$	[21]
6.0	0.1558	0.234(1)	0.387(3)	0.557(7)	$32^3 \times 64$	[22]
6.0	0.1558	0.229(2)	0.384(7)	0.555(12)	$24^3 \times 32$	this work
6.0	0.1563	0.1847(27)	0.353(15)	0.536(30)	$24^3 \times 54$	[21]
6.0	0.1563	0.185(1)	0.361(5)	0.506(11)	$32^3 \times 64$	[22]
6.0	0.1563	0.179(3)	0.358(11)	0.488(22)	$24^3 \times 32$	this work

TABLE VII. World Wilson fermion masses below $\beta=6.0$.

β	κ	am_π	am_ρ	am_N	Lattice	Ref.
5.93	0.1543	0.4572(26)	0.5527(40)	0.8674(102)	$24^3\times36$	[20]
5.93	0.1560	0.3573(19)	0.4864(42)	0.7448(99)	$24^3\times36$	[20]
5.93	0.1573	0.2641(25)	0.4369(48)	0.6423(80)	$24^3\times36$	[20]
5.93	0.1581	0.1885(31)	0.4071(57)	0.5652(92)	$24^3\times36$	[20]
5.85	0.1440	1.0293(12)	1.0598(15)	1.6961(50)	$24^3\times54$	[21]
5.85	0.1540	0.6122(11)	0.6931(27)	1.1060(55)	$24^3\times54$	[21]
5.85	0.1585	0.3761(12)	0.5294(69)	0.815(13)	$24^3\times54$	[21]
5.85	0.1585	0.378(2)	0.530(6)	0.783(10)	$16^3\times32$	[24]
5.85	0.1595	0.3088(14)	0.4856(96)	0.744(17)	$24^3\times54$	[21]
5.85	0.1600	0.2730(30)	0.486(9)	0.673(9)	$16^3\times32$	[24]
5.85	0.1605	0.2226(21)	0.434(20)	0.683(48)	$24^3\times54$	[21]
5.70	0.1600	0.6905(31)	0.8022(56)	1.3124(135)	$24^3\times32$	[20]
5.70	0.1600	0.6873(24)	0.8021(29)	1.2900(60)	$16^3\times20$	[25]
5.70	0.1610	0.6527(15)	0.7842(26)	1.263(5)	$12^3\times24$	[17]
5.70	0.1630	0.5621(18)	0.7232(35)	1.153(6)	$12^3\times24$	[17]
5.70	0.1640	0.5080(29)	0.6822(38)	1.0738(80)	$16^3\times20$	[25]
5.70	0.1650	0.4604(22)	0.6663(45)	1.039(8)	$12^3\times24$	[17]
5.70	0.1650	0.4589(22)	0.6491(73)	1.0301(104)	$24^3\times32$	[20]
5.70	0.1663	0.3829(26)	0.6206(103)	0.9421(131)	$24^3\times32$	[20]
5.70	0.1665	0.3674(39)	0.6085(58)	0.915(11)	$16^3\times20$	[25]
5.70	0.1670	0.3302(30)	0.6042(83)	0.919(14)	$12^3\times24$	[17]
5.70	0.1675	0.2955(24)	0.5912(125)	0.8668(177)	$24^3\times32$	[20]

The tadpole-improved value of κ_c that follows from this result is

$$\kappa_c=\frac{1}{8}\left[1+g^{*2}(0.025238-0.028989c_{SW}u_0^3\right.$$
$$\left.-0.012064(c_{SW}u_0^3)^2)\right]u_0^{-1}, \tag{10}$$

where c_{SW} is given by Eq. (3),

$$u_0=\left\langle\frac{1}{3}\,\mathrm{Tr}\,U_\square\right\rangle^{1/4} \tag{11}$$

and g^{*2} is the boosted coupling constant defined by

$$g^{*2}=g^2/u_0^4. \tag{12}$$

In Fig. 1 we compare the tadpole-improved perturbative formula (10) with the data where for the larger couplings we have taken u_0 from [14,15]. The curve and the data points agree within less than 1%. In Eq. (10) one has the choice of using the lowest order tadpole-improved value of c_{SW}, namely u_0^{-3} [4], or the value from Eq. (3) which is the value actually used in the simulations. Both procedures remove all the tadpole diagrams and differ only by small $O(g^4)$ terms, so they are both reasonable. We prefer the second choice.

We fit the other hadron masses by the formula

$$m_H^2=b_0+b_2m_\pi^2+b_3m_\pi^3, \quad H=\rho,N,\ldots . \tag{13}$$

The result of the fit is shown in Fig. 2 for both improved and Wilson fermion data. The Wilson fermion data are the world data compiled in Tables V, VI, and VII.

We find Eq. (13) to be a more appropriate fit formula than the ansatz [26]

$$m_H=b_0'+b_2'm_\pi^2+b_3'm_\pi^3, \tag{14}$$

because for the nucleon the plot of m_N^2 against m_π^2 (or $1/\kappa$) is less curved than m_N against m_π^2, as can be seen from comparing Fig. 2 with Fig. 3. [Note that the two formulas differ only by terms of $O(m_\pi^4)$]. This was noticed before in Refs.
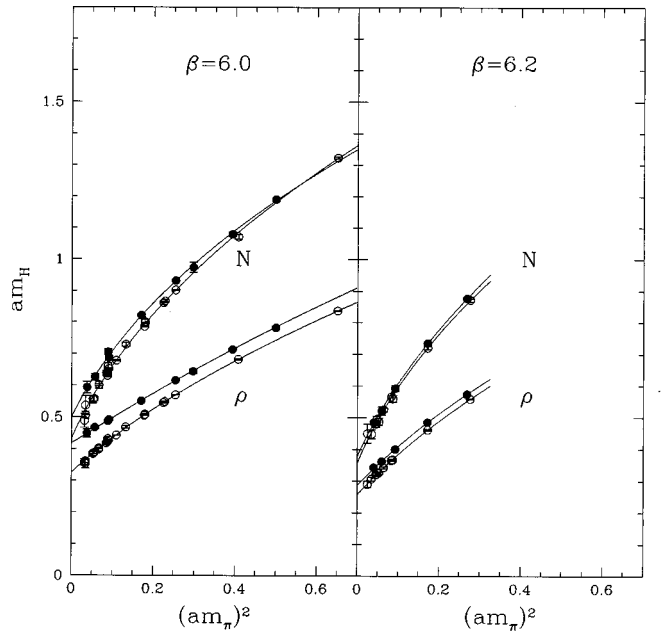

FIG. 3. Linear plot of ρ and nucleon masses for improved (●) and Wilson fermions (○).

TABLE VIII. Comparison of chiral extrapolations at $\beta=6.0$ using all the data (top rows), and using only the data from the largest lattice. In the fits on the $24^3 32$ lattice we have set $b_3 = b'_3 = 0$.

		$c_{SW}=0$		
V	Fit formulas	κ_c	am_ρ	am_N
$16^3 32$ & $24^3 32$	(8) & (13)	0.15713(3)	0.327(6)	0.412(16)
$24^3 32$	(6) & (13)	0.15709(4)	0.319(16)	0.377(37)
$24^3 32$	(6) & (14)	0.15709(4)	0.325(14)	0.410(26)
		$c_{SW}=1.769$		
V	Fit formulas	κ_c	am_ρ	am_N
$16^3 32$ & $24^3 32$	(8) & (13)	0.13531(1)	0.417(7)	0.511(15)
$24^3 32$	(6) & (13)	0.13526(2)	0.421(15)	0.514(27)
$24^3 32$	(6) & (14)	0.13526(2)	0.424(14)	0.527(23)

[16, 27], and recently also in Ref. [28]. To decide which fit formula is best and to do a reliable extrapolation to the chiral limit, it is important to have many κ values. For the a_0, a_1, and b_1 masses only a two-parameter fit with b_3 set to zero was reasonable. The mass values in the chiral limit for our data are also given in Tables I, II, and III.

We see that the effect of improvement is largest for the ρ mass. In the chiral limit the difference between improved and Wilson results is 25% at $\beta=6.0$ and still 12% at $\beta=6.2$. It is quite common to define the physical scale from the ρ mass. The relatively large change of this quantity from the Wilson to the improved case suggests that it contains large $O(a)$ corrections, and that this procedure is misleading. A better procedure is to use the string tension or r_0 [29], the force parameter, as the scale. For the nucleon mass the difference between the two actions is smaller.

At $\beta=6.0$ we have data on two different lattice sizes for improved and Wilson fermions. Though we have already seen that finite size effects are small, one may ask to do a separate analysis for each lattice size, to keep finite size and finite lattice spacing effects separate, and to test for consistency of the results. We have made fits using only the data on the large lattice. Because these data are closer to κ_c, the m_π^3 term in Eqs. (8), (13), and (14) is not needed, so that we have used the truncated formulae with b_3 and b'_3 set to zero. Near κ_c it should also make no difference whether Eq. (13) or Eq. (14) is used. The result of the fits are given in Table VIII. We see that the fits on the large lattice and the fit to all data points give consistent results for the masses. The errors from fitting just the data on the large lattice, however, turn out to be a factor of two larger. For κ_c the various fits give consistent results for Wilson fermions. For improved fermions the results differ by 2–3 standard deviations. The value from the simultaneous fit is the best estimate we have. It is in good agreement with the UKQCD result $\kappa_c=0.135335^{+20}_{-17}$ [30]. In the following we shall use the values from the simultaneous fits.

APE plots. In Figs. 4 and 5 we show the dimensionless ratio m_N/m_ρ as a function of $(m_\pi/m_\rho)^2$, a so-called APE plot, for $\beta=6.0$ and 6.2, both for improved and Wilson fermions (the latter using the world data given in Tables V and VI). The solid lines are the results of the ratio of the fits in
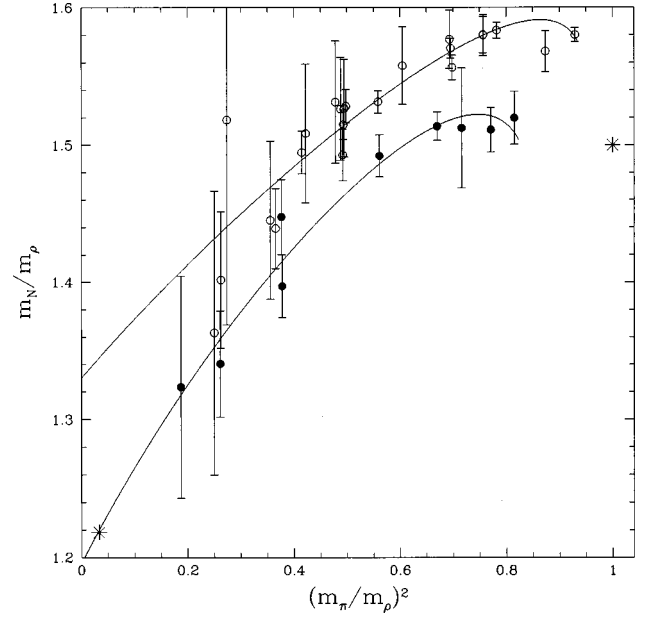

FIG. 4. *APE plot* at $\beta=6.0$ for improved (●) and Wilson fermions (○) compared with the physical mass ratio (∗) at the physical quark mass and in the heavy quark limit. The solid lines are from the mass fits described in the text.

Fig. 2. At $\beta=6.0$ we find that the mass ratio data are rather different for the two actions. The improved results lie consistently lower than the Wilson results. At $\beta=6.2$ we find the same pattern in the data.

At $\beta=6.0$ we can say something about the chiral limit. Our fits give $m_N/m_\rho=1.20(6)$ for improved fermions and $m_N/m_\rho=1.33(2)$ for Wilson fermions. The improved results come closer to the physical value than the Wilson results. At $\beta=6.2$ we are lacking data at small quark masses and on larger volumes. In the chiral limit our fits give $m_N/m_\rho=1.32(11)$ for improved fermions and $m_N/m_\rho=1.39(12)$
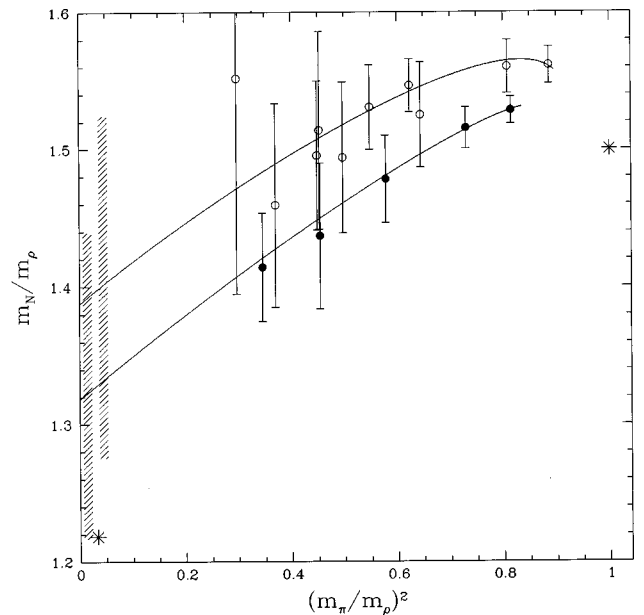

FIG. 5. The same as Fig. 4, but for $\beta=6.2$. The hatched bars indicate the errors of the fit in the chiral limit.

TABLE IX. The lattice spacing expressed in terms of the string tension K and the force parameter r_0. When several groups have computed these quantities, we have taken the weighted average, while we interpolate logarithmically whenever the values are not known.

β	$a\sqrt{K}$	Ref.	r_0/a	Ref.	$r_0\sqrt{K}$
6.8	0.0730(12)	[32]	16.7(4)	[15]	1.22(4)
6.5	0.1068(10)	[33]			
6.4	0.1215(12)	[32]	9.87(8)	[15]	
	0.1218(28)	[34]	9.70(24)	[34]	
	0.1215(11)	combined	9.85(8)	combined	1.197(15)
6.3	0.1394(11)	interpolated			
6.2	0.1610(9)	[35]	7.36(4)	[15]	
	0.1608(23)	[34]	7.33(25)	[34]	
	0.1609(28)	[36]			
	0.1610(8)	combined	7.36(4)	combined	1.185(9)
6.17	0.1677(8)	interpolated			
6.0	0.2209(23)	[35]	5.28(4)	[15]	
	0.2154(50)	[34]	5.53(15)	[34]	
	0.2182(21)	[37]			
	0.2191(15)	combined	5.30(4)	combined	1.161(12)
5.93	0.2536(29)	interpolated			
5.90	0.2702(37)	[38]	4.62(11)	[15]	1.25(3)
5.85	0.2986(27)	interpolated			
5.8	0.3302(30)	[38]	3.63(5)	[15]	1.199(20)
5.7	0.4099(24)	[38]	2.86(5)	[15]	1.172(22)
5.6			2.29(6)	[15]	
5.5			2.01(3)	[15]	

for Wilson fermions, so that we cannot say anything conclusive about the behavior of the two actions in the chiral limit in this case.

Scaling behavior. Let us now look at and compare the scaling behavior of the two actions. We shall limit our discussion to the ρ mass because the errors of the nucleon are too large to make precise statements. In order to exhibit the cutoff effects most clearly, it has been suggested [31] that m_ρ should be plotted in units of the square root of the string tension K which has cutoff errors of $O(a^2)$ only. In Table IX we have compiled the world string tension data. When there are several calculations, we performed the weighted average.

In Fig. 6 we plot the ratio $m_\rho/\sqrt{K}$ as a function of $a\sqrt{K}$. This is done for fixed physical π masses with $m_\pi^2 = 0$, $2K$, and $4K$. Comparing hadron masses at larger quark masses has the advantage that this does not require large extrapolations of the lattice data but rather involves small interpolations only. The Wilson fermion data shown are a fit to the world data compiled in Tables V, VI, and VII. As expected, the Wilson masses show practically a linear behavior in the lattice spacing a. We have done a simultaneous linear plus quadratic fit to the Wilson data and a quadratic fit to the improved data. The fit is constrained to agree in the continuum limit. The result of the fit is shown by the solid lines

in Fig. 6. In the continuum limit we obtain $m_\rho/\sqrt{K}$ $= 1.80(10)$. We compare this result with the experimental ρ mass. For the string tension we take the value

$$\sqrt{K} = 427 \text{ MeV} \tag{15}$$

which has been obtained from a potential fit to the charmonium mass spectrum [39]. Using this value the physical $m_\rho/\sqrt{K}$ is 1.80 which agrees with the lattice number.

The simultaneous fit uses all the information we have and gives the best estimate of the ratio $m_\rho/\sqrt{K}$ in the continuum limit. Separate fits to the improved and Wilson data give 1.64(13) and 2.01(15), respectively. These numbers are one standard deviation away from the result of the simultaneous fit. This shows that both data sets are important in the simultaneous fit, and that the error bar on the continuum result is substantially reduced by combining both data sets.

As mentioned previously, an alternative scale from the potential is r_0. We have also compiled lattice results for r_0 in Table IX. We see that it scales very well with $\sqrt{K}$, as the product $r_0\sqrt{K}$ is approximately constant at about 1.19, while the lattice spacing a changes by a factor of more than 5. However, the physical value of $r_0\sqrt{K}$ is 1.06, taking r_0^{-1} as 402 MeV which follows from the same potential that gives
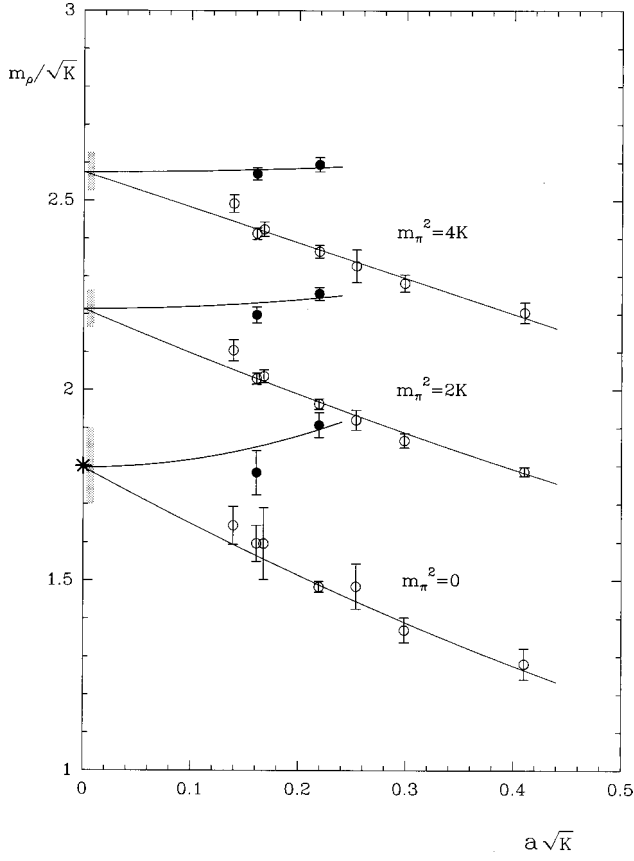
FIG. 6. The ratio $m_\rho/\sqrt{K}$ as a function of the lattice spacing for improved (●) and Wilson fermions (○). The solid lines are from a simultaneous linear plus quadratic fit to the Wilson data and a quadratic fit to the improved data. This is compared with the experimental value (∗) using $\sqrt{K}=427$ MeV. The shaded bars indicate the errors of the fit in the continuum limit.

$\sqrt{K}=427$ MeV [39]. It does not seem that this discrepancy will vanish as $a\to 0$. It is telling us that the lattice potential has a slightly different shape to the continuum potential. This may be an effect of quenching [40].

Although at $\beta=5.7$ we do not know the correct value of c_{SW}, using our larger value $c_{SW}=2.25$ we find $m_\rho/\sqrt{K}=1.94$ in the chiral limit. Comparing this number with Fig. 6, it indicates that $O(a^2)$ effects are moderate even at this coupling.

Mass splitting. The vector-pseudoscalar mass splitting

$$\Delta_{\text{V-PS}}=m_V^2-m_{\text{PS}}^2 \qquad (16)$$

is experimentally rather constant for all quark flavors. One finds

$$m_\rho^2-m_\pi^2=0.57 \text{ GeV}^2,$$

$$m_{K*}^2-m_K^2=0.55 \text{ GeV}^2,$$

$$m_{D*}^2-m_D^2=0.55 \text{ GeV}^2. \qquad (17)$$
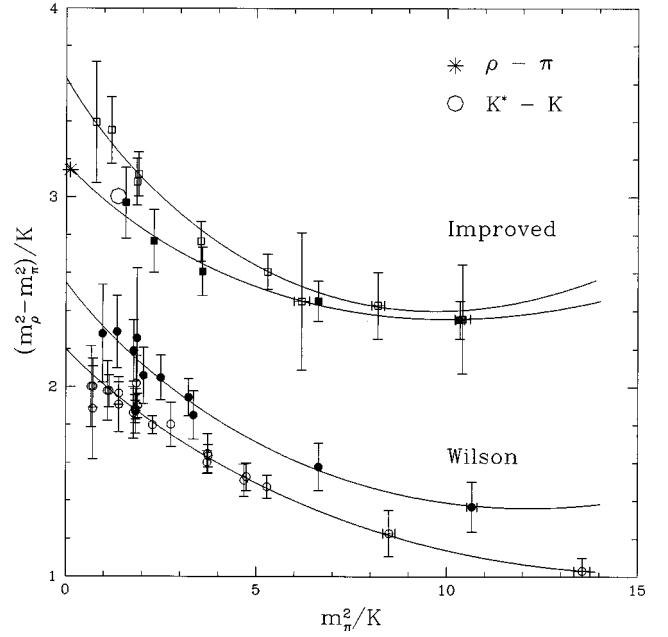
FIG. 7. The vector-pseudoscalar mass splitting as a function of the quark mass. Open symbols correspond to $\beta=6.0$, solid symbols to $\beta=6.2$. This is compared with the physical ρ-π (asterisk) and K^*-K (octogon) mass splitting. The curves are from the mass fits.

Quenched lattice calculations with Wilson fermions are unable to reproduce these numbers. Wilson fermions give a splitting which is much too small. In Fig. 7 we compare the experimental values of $m_\rho^2-m_\pi^2$ and $m_{K*}^2-m_K^2$ with the lattice data and the mass fits. As before, we have taken the string tension Eq. (15) as the scale. In Fig. 7 we also show the results for improved fermions and the corresponding mass fits as well. There is a noticeable change when going to the improved case. We find good agreement with experiment for the absolute values.

In the heavy quark effective theory [41]

$$\Delta_{\text{V-PS}}\propto\langle\bar\Psi\sigma_{\mu\nu}F_{\mu\nu}\Psi\rangle, \qquad (18)$$

where Ψ is the heavy quark field. So it is natural that turning on the Sheikholeslami-Wohlert term would increase the mass splitting, and this is what we see.

Wilson κ_c. Let us now come back to the critical value of κ for Wilson fermions. In Table X we have given the values of κ_c from a fit of the world data in Tables V, VI, and VII

TABLE X. The critical values of κ, κ_c, for the Wilson world data.

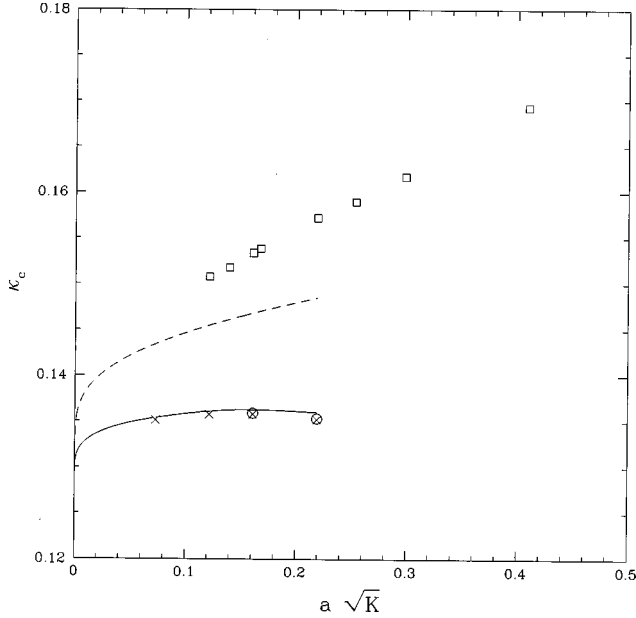| β	κ_c
6.40	0.150759(145)
6.30	0.151774(36)
6.20	0.153374(17)
6.17	0.153838(37)
6.00	0.157211(8)
5.93	0.158985(73)
5.85	0.161716(23)
5.70	0.169313(72)

FIG. 8. The critical value of κ as a function of the lattice spacing for Wilson fermions ($\square$). The dashed curve is the prediction of tadpole improved perturbation theory. This is compared with the results for improved fermions from Fig. 1.

using the phenomenological ansatz (8). In Fig. 8 we plot these results as a function of $a\sqrt{K}$ (the string tension being taken from Table IX). We see that κ_c is a linear function of a over the whole range of the data which extends from $\beta = 5.7$ to 6.4. Comparing this with the improved κ_c, which is approximately constant, we conclude that the Wilson κ_c has large $O(a)$ effects. We also compare the Wilson data with the predictions of tadpole-improved perturbation theory as given by Eq. (10) with $c_{SW} = 0$. Here we have taken the one-loop perturbative formula for a beyond $\beta = 6.8$ where there are no numerical values for the string tension available any more. Not even at the smallest value of a can perturbation theory describe the Wilson data. For improved fermions, on the other hand, the agreement with tadpole-improved perturbation theory is quite good, as we have already noticed.

IV. QUARK MASSES

We shall now turn to the calculation of the quark masses. When chiral symmetry is dynamically broken, care has to be taken in defining renormalized masses. In the continuum the renormalized quark mass at scale $p^2 = \mu^2$ can be written [42]

$$\frac{1}{4} \mathrm{Tr}[S_F^{-1}(m) - S_F^{-1}(0)] = m(\mu), \qquad (19)$$

where S_F is the renormalized quark propagator which is to be evaluated in a given gauge. This definition refers to the momentum subtraction scheme. It is usual to give the quark masses in the modified minimal subtraction scheme ($\overline{\mathrm{MS}}$). To convert from one scheme to the other, one has to go to high enough scales so that one can use perturbation theory. If the quark mass is defined in this way, then the renormalized mass is proportional to the bare mass.

On the lattice the standard assignment of the bare mass is

$$am(a) = \frac{1}{2}\left(\frac{1}{\kappa} - \frac{1}{\kappa_c}\right), \qquad (20)$$

giving the renormalized mass as

$$m^{\overline{\mathrm{MS}}}(\mu) = Z_m^{\overline{\mathrm{MS}}}(a\mu, am)m(a), \qquad (21)$$

where $Z_m^{\overline{\mathrm{MS}}}(a\mu, am)$ is the mass renormalization constant. We call this method of determining the renormalized mass the standard method.

An alternative way of defining a bare mass is by means of the PCAC (partial conservation of axial vector current) relation between the divergence of the axial vector current $A_\mu = \bar{\psi}\gamma_\mu\gamma_5\psi$ and the pseudoscalar density $P = \bar{\psi}\gamma_5\psi$,

$$\widetilde{m}(a) = \frac{\partial_4\langle A_4(x)\mathcal{O}\rangle}{2\langle P(x)\mathcal{O}\rangle}, \qquad (22)$$

where $\mathcal{O}$ is a suitable operator having zero three-momentum and no physical overlap with $A_4(x)$ and $P(x)$ to avoid contact terms. (See later on for a precise definition.) All operators are bare operators. To avoid anomaly terms in Eq. (22), flavor nonsinglet operators are taken. We call this method the Ward identity method. The renormalized mass is then given by

$$m^{\overline{\mathrm{MS}}}(\mu) = \frac{Z_A(am)}{Z_P^{\overline{\mathrm{MS}}}(a\mu, am)}\,\widetilde{m}(a), \qquad (23)$$

where $Z_A(am)$ and $Z_P^{\overline{\mathrm{MS}}}(a\mu, am)$ are the renormalization constants of the axial vector current and the pseudoscalar density, respectively.

The quark mass inherits its scale dependence from the renormalization constants Z_m and Z_P which involve logarithms of μ. In the following we will compute Z_m and Z_P perturbatively to one-loop order for lack of a better, nonperturbative determination. To keep the logarithms under control it is best to take $a\mu = 1$ and do the transformation to any other scale by the renormalization group formula

$$m^{\overline{\mathrm{MS}}}(\mu') = \left(\frac{\alpha_s^{\overline{\mathrm{MS}}}(\mu')}{\alpha_s^{\overline{\mathrm{MS}}}(\mu)}\right)^{8/22} m^{\overline{\mathrm{MS}}}(\mu). \qquad (24)$$

In the continuum limit both procedures should give identical results for $m^{\overline{\mathrm{MS}}}(\mu)$. Note, however, that the two bare masses m and $\widetilde{m}$ can be different, though they both vanish in the chiral limit. On the lattice the two procedures may give different results for $m^{\overline{\mathrm{MS}}}(\mu)$ due to nonuniversal discretization errors.

The lattice calculation of the quark masses now proceeds in two steps. In the first step one has to find the κ values corresponding to the real world by adjusting, e.g., the pseudoscalar meson masses to their experimental numbers. In case of the Ward identity method one furthermore has to compute $\widetilde{m}$. In the second step the bare quark masses have to be converted to renormalized masses. We shall compute the masses of the u and d quarks, which we assume to be equal, and the mass of the strange (s) quark.
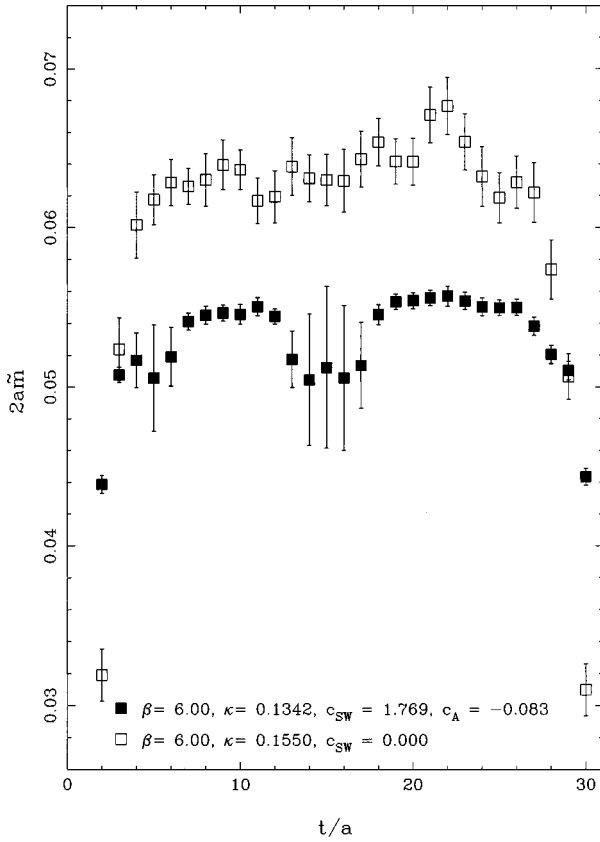
FIG. 9. The bare mass $\widetilde{m}$ from the Ward identity method at $\beta = 6.0$ for Wilson ($\square$) and improved fermions ($\blacksquare$) on the $16^3 32$ lattice. The errors are bootstrap errors.

Improved fermions. Let us consider the case of improved fermions first. Later on we shall compare our results with the predictions of Wilson fermions to see the effect of improvement.

We will discuss the Ward identity method first. For the operator $\mathcal{O}$ we take the pseudoscalar density

$$P(0) = \sum_{\vec{x}} P(x_4 = 0, \vec{x}) \tag{25}$$

and smear it as we did in the hadron mass calculations. As the $P(0)$ part is common to all two-point functions, we could have used any operator projecting onto the pseudoscalar state. Similarly, we write

$$A_4(t) = \sum_{\vec{x}} A_4(x_4 = t, \vec{x}). \tag{26}$$

For improved fermions the axial vector current in Eq. (22) is to be replaced by

$$A_4 \rightarrow A_4 + c_A a \, \partial_4 P(x), \tag{27}$$

where c_A is a function of the coupling only. The time derivative ∂_4 is taken to be the average of the forward and backward derivative. The coefficient c_A has been computed in [4] giving $c_A = -0.083$ at $\beta = 6.0$ and $c_A = -0.037$ at $\beta = 6.2$. The resulting bare mass
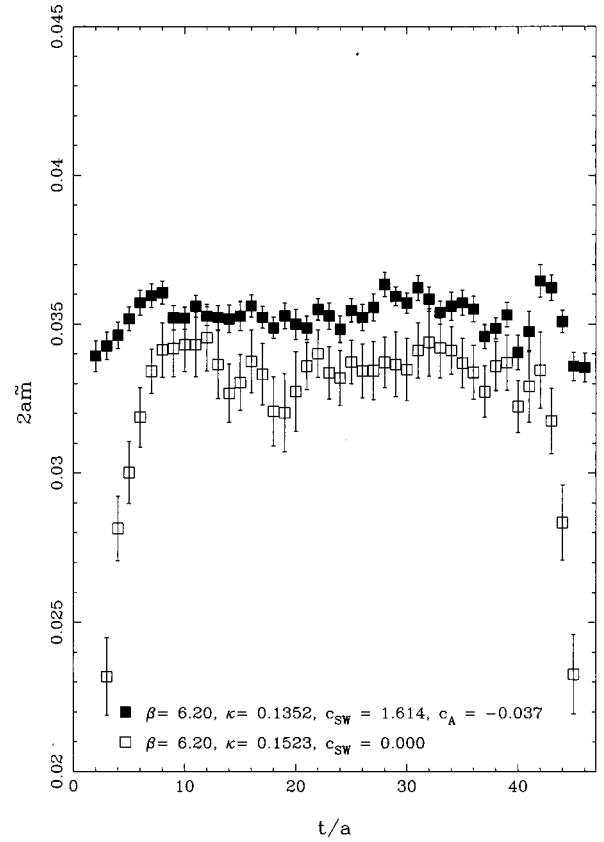

FIG. 10. The same as Fig. 9 but for $\beta = 6.2$ for Wilson ($\square$) and improved fermions ($\blacksquare$).

$$\widetilde{m}(a) = \frac{\partial_4 \langle A_4(t) P(0) \rangle + c_A a \partial_4^2 \langle P(t) P(0) \rangle}{2 \langle P(t) P(0) \rangle} \tag{28}$$

has been plotted in Fig. 9 for $\beta = 6.0$ and our smallest quark mass on the $16^3 32$ lattice. In Fig. 10 we show the same quantity for $\beta = 6.2$ and our smallest quark mass on the $24^3 48$ lattice. (Also shown in these figures are the results for Wilson fermions which we will discuss later on.) Equation (28) should be independent of t, except where the operators physically overlap with the source, if the cutoff effects have been successfully removed. In both cases, but in particular at $\beta = 6.2$, we see a smaller deviation from the plateau at small and large t values. To obtain the mass, we fit the ratio (28) to a constant. We have used the same fit ranges as for the pion mass. The results of the fit are given in Tables XI and XII. At $\beta = 6.0$ in the improved case we see that at $\kappa = 0.1342$ we have small finite size effects, indicating again that our results on the $16^3 32$ lattice are not significantly volume dependent.

For both the Ward identity and the standard method we choose to determine the κ values from the pseudoscalar meson masses. Sometimes the $\phi(1020)$ meson is taken for the determination of the strange quark mass. However, we do not think that this is a good idea because of potential ω-ϕ mixing [43]. We generalize Eq. (8) to the case of two different quark masses by writing

$$\frac{1}{2} \left(\frac{1}{\kappa_1} + \frac{1}{\kappa_2} \right) - \frac{1}{\kappa_c} = b_2 m_{\text{PS}}^2 + b_3 m_{\text{PS}}^3 \tag{29}$$

TABLE XI. The bare quark masses $\widetilde{m}$ for Wilson fermions ($c_{SW}=0$) and improved fermions ($c_{SW}=1.769$) at $\beta=6.0$. The errors are bootstrap errors.

| | $\beta=6.0$ | |
| | $c_{SW}=0$ | |
V	κ	$2a\widetilde{m}$
	0.1487	0.2959(5)
	0.1515	0.1866(5)
$16^3 32$	0.1530	0.1321(5)
	0.1550	0.0642(7)
	$c_{SW}=1.769$	
V	κ	$2a\widetilde{m}$
	0.1300	0.2836(3)
	0.1310	0.2279(3)
$16^3 32$	0.1324	0.15231(10)
	0.1333	0.10380(11)
	0.1342	0.0553(2)
	0.1342	0.0551(3)
$24^3 32$	0.1346	0.0330(3)
	0.1348	0.0214(4)

TABLE XII. The bare quark masses $\widetilde{m}$ for Wilson fermions ($c_{SW}=0$) and improved fermions ($c_{SW}=1.614$) at $\beta=6.2$. The errors are bootstrap errors.

| | $\beta=6.2$ | |
| | $c_{SW}=0$ | |
V	κ	$2a\widetilde{m}$
	0.1468	0.2474(3)
	0.1489	0.1616(3)
$24^3 48$	0.1509	0.0845(3)
	0.1518	0.0514(3)
	0.1523	0.0336(3)
	$c_{SW}=1.614$	
V	κ	$2a\widetilde{m}$
	0.1321	0.21618(7)
	0.1333	0.14585(7)
$24^3 48$	0.1344	0.08185(7)
	0.1349	0.05283(8)
	0.1352	0.03538(9)

with the same coefficients b_2, b_3 as before. This is inspired by chiral perturbation theory where it is expected that the pseudoscalar mass is a function of the sum of quark and antiquark mass $m_q + m_{\bar{q}}$ even when quark and antiquark have different flavors. By fixing m_{PS} to the physical pion mass $m_{\pi^\pm}$, using the string tension values compiled in Table IX with Eq. (15) as the scale, we find the value for $\kappa_{u,d}=\kappa_1 \equiv \kappa_2$. The strange quark mass is obtained by identifying m_{PS} with the kaon mass $m_{K^\pm}$, taking $\kappa_1=\kappa_{u,d}$ as input and solving for $\kappa_2=\kappa_s$. This gives for the light mass

$$m_{u,d}a = \frac{1}{2}\left(\frac{1}{\kappa_{u,d}}-\frac{1}{\kappa_c}\right)= \begin{cases} 0.001836(36) & \text{for } \beta=6.0, \\ 0.001384(36) & \text{for } \beta=6.2. \end{cases} \tag{30}$$

For the strange mass we get

$$m_s a = \frac{1}{2}\left(\frac{1}{\kappa_s}-\frac{1}{\kappa_c}\right)= \begin{cases} 0.0419(11) & \text{for } \beta=6.0, \\ 0.0310(11) & \text{for } \beta=6.2, \end{cases} \tag{31}$$

where $m_{u,d}=1/2(m_u+m_d)$.

The bare masses $\widetilde{m}_{u,d},\widetilde{m}_s$ are computed analogously. We write

$$\widetilde{m}\equiv\frac{1}{2}(\widetilde{m}_1+\widetilde{m}_2)=\widetilde{b}_2 m_{PS}^2+\widetilde{b}_3 m_{PS}^3. \tag{32}$$

Using this parametrization we first fit the masses in Tables XI and XII to the pseudoscalar masses in Tables II and III. This gives us $\widetilde{b}_2, \widetilde{b}_3$. We then determine $\widetilde{m}_{u,d},\widetilde{m}_s$ by fixing m_{PS} to the physical pion and kaon masses, respectively, as before.

The mass dependence of the renormalization constant $Z_A(am)$ can be parametrized as [44]

$$Z_A(am)=(1+b_A am)Z_A. \tag{33}$$

The renormalization constant Z_A has been computed nonperturbatively in Ref. [45]. The fit formula in this paper gives $Z_A=0.7924$ at $\beta=6.0$ and $Z_A=0.8089$ at $\beta=6.2$. The coefficient b_A is only known perturbatively to one-loop order [46]. The best we can do at present is to take the tadpole-improved value. For the boosted coupling we use $\alpha_s^{\overline{MS}}(1/a)$, giving

$$b_A=1+\alpha_s^{\overline{MS}}(1/a)1.912, \tag{34}$$

where we take $\alpha_s^{\overline{MS}}(1/a)=0.1981$ at $\beta=6.0$ and $\alpha_s^{\overline{MS}}(1/a)=0.1774$ at $\beta=6.2$ [14]. For $Z_P^{\overline{MS}}(a\mu,am)$ we write

$$Z_P^{\overline{MS}}(a\mu,am)=(1+b_P am)Z_P^{\overline{MS}}(a\mu). \tag{35}$$

The renormalization constant $Z_P^{\overline{MS}}(a\mu)$ has been computed perturbatively [47]. The result is

$$Z_P^{\overline{MS}}(a\mu)=1-\frac{g^2}{16\pi^2}C_F[-6\ln(a\mu)+22.595-2.249c_{SW}$$
$$+2.036c_{SW}^2], \tag{36}$$

with $C_F=4/3$. We shall take the scale $\mu=1/a$ and use the tadpole-improved value of Eq. (36) which turns out to be

$$Z_P^{\overline{MS}}(a\mu=1)=\left[1-\frac{a_s^{\overline{MS}}(1/a)}{4\pi}[16.967-2.999c_{SW}u_0^3$$
$$+2.715(c_{SW}u_0^3)^2]\right]u_0. \tag{37}$$

(We use $u_0=0.8778$ at $\beta=6.0$ and $u_0=0.8851$ at $\beta=6.2$.) The coefficient b_P has also been computed perturbatively to one-loop order [46]. Again we shall use the tadpole improved value

$$b_P=1+\alpha_s^{\overline{MS}}(1/a)1.924. \tag{38}$$

TABLE XIII. Our results of the renormalized quark masses $m^{\overline{\text{MS}}}(2\text{ GeV})$ in MeV for improved and Wilson fermions, together with the extrapolation to the continuum limit ($\beta = \infty$). The continuum numbers refer to improved fermions. We give the results for both the Ward identity and the standard method.

β	c_{SW}	$m_{u,d}^{\overline{\text{MS}}}$		$m_s^{\overline{\text{MS}}}$	
		Ward	Standard	Ward	Standard
6.0	0	4.40 ± 0.17	6.47 ± 0.20	105.0 ± 4.5	141.8 ± 6.0
6.2	0	4.73 ± 0.14	6.39 ± 0.25	108.5 ± 4.2	138.8 ± 7.4
6.0	1.769	4.02 ± 0.10	4.94 ± 0.09	92.8 ± 2.9	109.4 ± 3.9
6.2	1.614	4.47 ± 0.06	5.09 ± 0.16	101.6 ± 1.7	111.7 ± 4.7
∞		5.00 ± 0.18	5.27 ± 0.36	111.9 ± 5.0	114.4 ± 11.1

We cannot be sure that we have removed all $O(a)$ effects in Z_P. Therefore we have also computed the renormalization constants $Z_A(am)$, $Z_P(a\mu,am)$ nonperturbatively [48]. So far we have results for $\beta = 6.0$ only. Our numbers are in fair agreement with the nonperturbative calculation in Ref. [45] and the tadpole-improved value (37). However, for small μ the constant Z_P behaves very differently from the perturbative formula.

To compare the results at the two different β values, we rescale them both to $\mu' = 2$ GeV using formula (24). As before, we use the string tension to convert the lattice spacing into physical units. The resulting quark masses $m_{u,d}^{\overline{\text{MS}}}(2\text{ GeV})$, $m_s^{\overline{\text{MS}}}(2\text{ GeV})$ are given in Table XIII.

Let us now discuss the standard method. We already have determined $m_{u,d}(a), m_s(a)$ in Eqs. (30) and (31). For the renormalization constant $Z_m^{\overline{\text{MS}}}(a\mu,am)$ we write

$$Z_m^{\overline{\text{MS}}}(a\mu,am) = (1 + b_m am) Z_m^{\overline{\text{MS}}}(a\mu). \tag{39}$$

The constant $Z_m^{\overline{\text{MS}}}(a\mu)$ has been computed perturbatively [47]. We obtain

$$Z_m^{\overline{\text{MS}}}(a\mu) = 1 - \frac{g^2}{16\pi^2} C_F [6\ln(a\mu) - 12.952 - 7.738 c_{\text{SW}} + 1.380 c_{\text{SW}}^2]. \tag{40}$$

The tadpole-improved value, which we will be using, is

$$Z_m^{\overline{\text{MS}}}(a\mu = 1) = \left[1 - \frac{\alpha_s^{\overline{\text{MS}}}(1/a)}{4\pi} \left[-4.110 - 10.317 c_{\text{SW}} u_0^3 + 1.840 (c_{\text{SW}} u_0^3)^2 \right] \right] u_0^{-1}. \tag{41}$$

The coefficient b_m has been computed in [46]. The tadpole-improved value is

$$b_m = -\frac{1}{2} - \alpha_s^{\overline{\text{MS}}}(1/a)1.210. \tag{42}$$

Again we extrapolate the quark masses to $\mu' = 2$ GeV using Eq. (24). The results which follow from this approach are listed in Table XIII as well.

The results of the Ward identity and the standard method may differ by $O(a^2)$ effects, and they do. We can "fit" the a dependence by

$$m_q^{\overline{\text{MS}}} = c_0 + c_2 a^2. \tag{43}$$

The result of the fit is shown in Figs. 11 and 12. The continuum values from this fit are given in Table XIII. We find that the two methods give consistent results in the continuum limit. Taking the statistical average of the two results we obtain the continuum values

$$m_{u,d}^{\overline{\text{MS}}}(2\text{ GeV}) = 5.1 \pm 0.2 \text{ MeV}, \tag{44}$$

$$m_s^{\overline{\text{MS}}}(2\text{ GeV}) = 112 \pm 5 \text{ MeV}. \tag{45}$$

The Ward identity method appears to have larger $O(a^2)$ effects than the standard method.

We may compare our results with the prediction of chiral perturbation theory, which cannot give absolute values but can determine the ratio of m_s to $m_{u,d}$. A recent calculation gives [49] $m_s/m_{u,d} = 24.4 \pm 1.5$. We find $m_s/m_{u,d} = 22.2 \pm 1.2$.
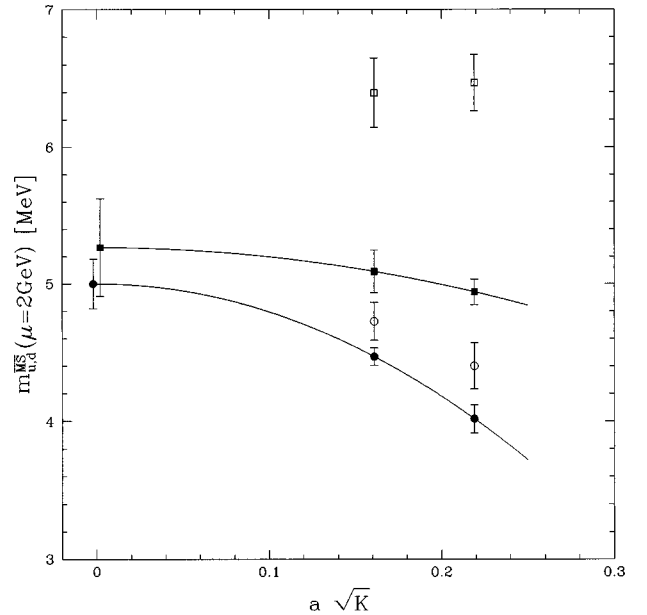

FIG. 11. The light quark mass $m_{u,d}^{\overline{\text{MS}}}$ as a function of the lattice spacing for improved fermions using the Ward identity (●) and standard method (■). This is compared with the Wilson result for the Ward identity (○) and standard method (□). The curves are quadratic extrapolations to the continuum limit.
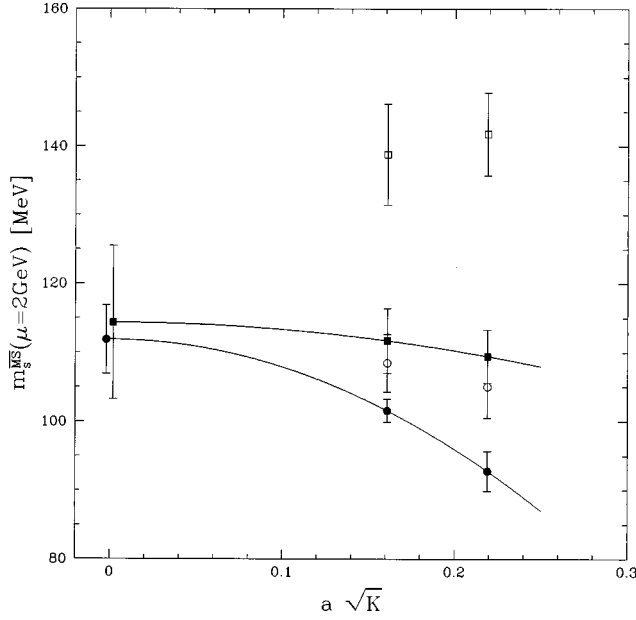
FIG. 12. The same as Fig. 11 but for the strange quark mass $m_s^{\overline{\mathrm{MS}}}$.

Wilson fermions. Let us now consider the case of Wilson fermions. We proceed in the same way as before. The situation here is that $Z_A(am)$ is known nonperturbatively only for $\beta = 6.0$ [50], and that b_A, b_P, and b_m are only known to the tree level. So for Z_A we use the tadpole-improved perturbative value

$$Z_A = \left[1 - \frac{\alpha_s^{\overline{\mathrm{MS}}}(1/a)}{4\pi} 7.901 \right] u_0, \qquad (46)$$

and for b_A, b_P, and b_m we take the tree-level results. Comparing Z_A with the nonperturbative determination at $\beta = 6.0$
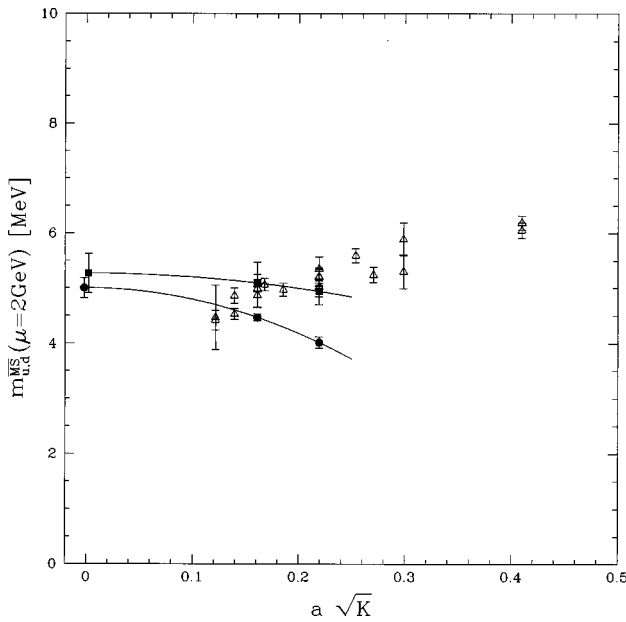
FIG. 13. The light quark mass $m_{u,d}^{\overline{\mathrm{MS}}}$ for improved fermions from Fig. 11 compared with the world Wilson masses ($\triangle$) compiled in [52].
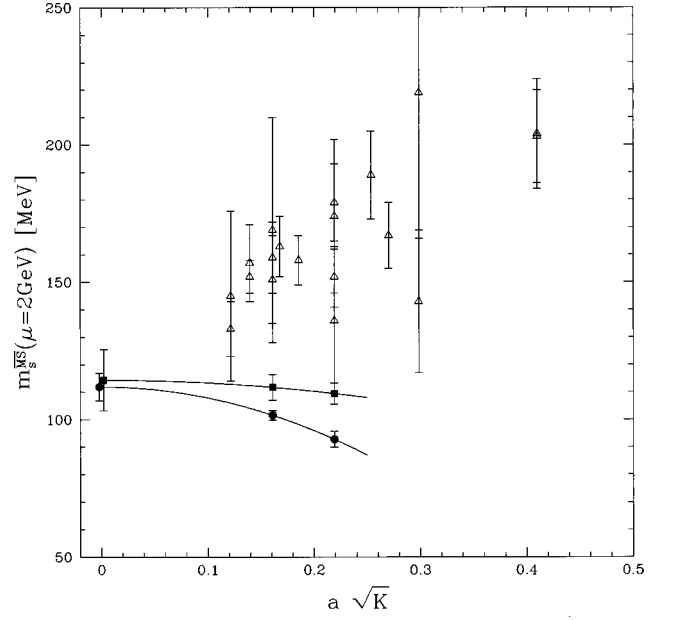

FIG. 14. The strange quark mass $m_s^{\overline{\mathrm{MS}}}$ for improved fermions from Fig. 12 compared with the world Wilson masses ($\triangle$) compiled in [52]. These authors use the $\phi(1020)$ meson to determine the strange quark mass.

[50], as well as with a nonperturbative calculation at $\beta = 5.9$, 6.1, and 6.3 using the Ward identity [51], we find good agreement. The renormalization constants $Z_P^{\overline{\mathrm{MS}}}(a\mu = 1)$ and $Z_m^{\overline{\mathrm{MS}}}(a\mu = 1)$ are obtained from Eqs. (37) and (41) by setting $c_{\mathrm{SW}} = 0$. The resulting quark masses are given in Table XIII, and they are plotted and compared with the improved results in Figs. 11 and 12. In this case we expect discretization errors of $O(a)$ instead of $O(a^2)$. So it is not surprising that the Ward identity and the standard method give results which are far apart. We find that the Ward identity method gives mass values which are closer to the continuum result.

Finally, in Figs. 13 and 14 we compare our improved quark masses with the world data of Wilson quark masses as compiled in Ref. [52] for the standard method. These authors use the ρ mass extrapolated to the chiral limit to set the scale. At $\beta = 6.0$ the scale set by the string tension and by the Wilson action ρ mass differ by about 20% which explains the difference between our Wilson data and the world data in Figs. 13 and 14. We see that the improved action improves the scaling behavior.

V. DECAY CONSTANTS

The pion decay constant f_π is well known experimentally and can be determined from the two-point correlation functions on the lattice as well, allowing for a further test of scaling of the improved theory. We shall also look at the decay constants of the K, ρ, K^*, and the a_1 meson.

In Euclidean space at zero three-momentum we define

$$\langle 0|\mathcal{A}_4|\pi\rangle = m_\pi f_\pi,$$

$$\langle 0|\mathcal{A}_i|a_1,\lambda\rangle = e(\lambda)_i m_{a_1}^2 f_{a_1}, \qquad (47)$$

$$\langle 0|\mathcal{V}_i|\rho,\lambda\rangle = e(\lambda)_i \frac{m_\rho^2}{f_\rho},$$

where $\mathcal{A}$ and $\mathcal{V}$ are the renormalized axial vector and vector current, respectively, and $e(\lambda)$ is the polarization vector with $\sum_\lambda e_i^*(\lambda)e_j(\lambda) = \delta_{ij}$. The pseudoscalar and vector states are normalized by

$$\langle p|p'\rangle = (2\pi)^3 2p_0 \delta(\vec{p}-\vec{p}'). \tag{48}$$

Note that our f_{a_1} is defined to be dimensionless.

In the improved theory the renormalized operators are

$$\mathcal{A}_\mu = (1+b_A am)Z_A(A_\mu + c_A a\partial_\mu P), \tag{49}$$

$$\mathcal{V}_\mu = (1+b_V am)Z_V(V_\mu + ic_V a\partial_\lambda T_{\mu\lambda}), \tag{50}$$

where $V_\mu = \bar{\psi}\gamma_\mu\psi$ and $T_{\mu\nu} = \bar{\psi}\sigma_{\mu\nu}\psi$ are the vector and tensor operators, respectively. We use the definition $\sigma_{\mu\nu} = i[\gamma_\mu,\gamma_\nu]/2$. Both currents are (partially) conserved, and hence no scale enters into their definition. The renormalization constant Z_A and the improvement coefficients c_A and b_A have already been given in the last section. The renormalization constant Z_V and the coefficients b_V and c_V have been computed nonperturbatively in Refs. [45, 53]. At $\beta=6.0$ the values are $Z_V=0.7780$, $b_V=1.472$, and $c_V=-0.32(6)$, and at $\beta=6.2$ the numbers are $Z_V=0.7927$, $b_V=1.409$, and $c_V=-0.22(7)$. While for most of these quantities the authors have given fit formulas in g^2, for c_V we have read the numbers from the graph in [53], as no such formula exists yet. We have also determined Z_V and b_V at $\beta=6.0$ from our nucleon three-point functions and find consistent results.

On the lattice we extract the meson decay constant from two-point correlation functions. For large times we expect that

$$C_{\mathcal{O}_1\mathcal{O}_2}(t) = \langle\mathcal{O}_1(t)\mathcal{O}_2^\dagger(0)\rangle$$
$$= \frac{1}{2m_H}[\langle 0|\mathcal{O}_1|H\rangle\langle 0|\mathcal{O}_2|H\rangle^* e^{-m_H t}$$
$$+ \langle 0|\mathcal{O}_1^\dagger|H\rangle^*\langle 0|\mathcal{O}_2^\dagger|H\rangle e^{-m_H(T-t)}]$$
$$\equiv A_{\mathcal{O}_1\mathcal{O}_2}[e^{-m_H t} + \eta_1\eta_2 e^{-m_H(T-t)}], \tag{51}$$

where $\mathcal{O}(t)$ is of the form $V_s^{-1/2}\sum_{\vec{x}}\bar{\psi}(\vec{x},t)\Gamma\psi(\vec{x},t)$, V_s being the spatial volume of the lattice, and $\mathcal{O}^\dagger = \eta\mathcal{O}$ with $\eta=\pm 1$ being given by $\gamma_4\Gamma^\dagger\gamma_4 = \eta\Gamma$. The η factor tells us how $\mathcal{O}$ behaves under time reversal, i.e., whether the two-point function is symmetric or antisymmetric with respect to $t \to T-t$. Here T is the temporal extent of the lattice. In general we have computed correlation functions with local (L) and smeared (S) operators.

We shall now consider the appropriate matrix elements separately. We start with those matrix elements necessary for the π. With our conventions we set

$$\langle 0|A_4|\pi\rangle = m_\pi f_\pi^{(0)},$$
$$\langle 0|a\partial_4 P|\pi\rangle = -\sinh am_\pi\langle 0|P|\pi\rangle$$
$$= m_\pi a f_\pi^{(1)}, \tag{52}$$

where $f^{(0)}, f^{(1)}$ are defined to be real and positive. By computing $C_{A_4 P}^{LS}$ and C_{PP}^{SS} we find, for the matrix element of A_4 from Eq. (52),

$$m_\pi f_\pi^{(0)} = -2\kappa\frac{\sqrt{2m_\pi}A_{A_4 P}^{LS}}{\sqrt{A_{PP}^{SS}}}, \tag{53}$$

and for the matrix element of $\partial_4 P$ we obtain from the ratio of the C_{PP}^{LS} and $C_{A_4 P}^{LS}$ correlation functions

TABLE XIV. The various contributions to the decay constants f_π, f_ρ, and f_{a_1} at $\beta=6.0$.

			$\beta=6.0$ $c_{SW}=0$			
V	κ	$af_\pi^{(0)}$	-	$f_\rho^{(0)}$	-	$f_{a_1}^{(0)}$
	0.1487	0.136(2)		0.305(5)		0.161(5)
$16^3 32$	0.1515	0.122(2)		0.364(5)		0.207(3)
	0.1530	0.113(2)		0.397(7)		0.231(3)
	0.1550	0.098(2)		0.459(9)		0.262(4)
			$c_{SW}=1.769$			
V	κ	$af_\pi^{(0)}$	$af_\pi^{(1)}/f_\pi^{(0)}$	$f_\rho^{(0)}$	$af_\rho^{(1)}/f_\rho^{(0)}$	$f_{a_1}^{(0)}$
	0.1300	0.1341(15)	1.792(7)	0.209(9)	0.670(2)	0.131(7)
	0.1310	0.1295(15)	1.698(8)	0.228(3)	0.588(2)	0.153(13)
$16^3 32$	0.1324	0.1204(8)	1.599(5)	0.261(2)	0.4823(12)	0.172(7)
	0.1333	0.1128(9)	1.541(3)	0.288(3)	0.4147(15)	0.202(16)
	0.1342	0.1037(8)	1.511(6)	0.323(3)	0.353(2)	0.208(16)
	0.1342	0.105(2)	1.521(16)	0.330(7)	0.348(3)	0.212(10)
$24^3 32$	0.1346	0.101(2)	1.58(3)	0.352(7)	0.327(6)	0.225(14)
	0.1348	0.100(3)	1.62(5)	0.352(15)	0.324(19)	0.25(2)

TABLE XV. The same as Table XIV but for $\beta = 6.2$.

			$\beta = 6.2$		
			$c_{SW} = 0$		
V	κ	$af_\pi^{(0)}$		$f_\rho^{(0)}$	$f_{a_1}^{(0)}$
	0.1468	0.1025(19)		0.268(5)	0.127(9)
	0.1489	0.0930(17)		0.315(6)	0.180(4)
$24^3 48$	0.1509	0.0798(14)		0.376(7)	0.230(4)
	0.1518	0.0719(13)		0.412(9)	0.261(4)
	0.1523	0.0669(14)		0.438(10)	0.276(5)
			$c_{SW} = 1.614$		
V	κ	$af_\pi^{(0)}$	$af_\pi^{(1)}/f_\pi^{(0)}$	$f_\rho^{(0)}$	$af_\rho^{(1)}/f_\rho^{(0)}$	$f_{a_1}^{(0)}$
	0.1321	0.0985(11)	1.297(3)	0.211(3)	0.4637(8)	0.133(2)
	0.1333	0.0913(11)	1.198(4)	0.243(3)	0.3719(10)	0.167(2)
$24^3 48$	0.1344	0.0818(10)	1.133(2)	0.283(4)	0.2900(15)	0.204(3)
	0.1349	0.0758(9)	1.118(7)	0.308(5)	0.255(2)	0.226(3)
	0.1352	0.072(3)	1.131(11)	0.327(16)	0.235(4)	0.241(11)

$$\frac{af_\pi^{(1)}}{f_\pi^{(0)}} = \sinh am_\pi \frac{A_{PP}^{LS}}{A_{A_4 P}^{LS}}. \qquad (54)$$

Alternatively, we can take the time derivative from the plateau in the correlation function. Numerically we found that it made very little difference to the result.

For the a_1 we set

$$\langle 0|A_i|a_1, \lambda \rangle = e(\lambda)_i m_{a_1}^2 f_{a_1}^{(0)}, \qquad (55)$$

and we find

$$m_{a_1}^2 f_{a_1}^{(0)} = 2\kappa \frac{\sqrt{2m_{a_1}} \Sigma_k A_{A_k A_k}^{LS}}{\sqrt{3\Sigma_k A_{A_k A_k}^{SS}}}. \qquad (56)$$

For the ρ we set

$$\langle 0|V_i|\rho, \lambda \rangle = e(\lambda)_i m_\rho^2 f_\rho^{(0)}, \qquad (57)$$

$$\langle 0|a\partial_4 T_{i4}|\rho, \lambda \rangle = -\sinh am_\rho \langle 0|T_{i4}|\rho, \lambda \rangle = ie(\lambda)_i m_\rho^2 af_\rho^{(1)},$$

and we obtain

$$m_\rho^2 f_\rho^{(0)} = 2\kappa \frac{\sqrt{2m_\rho} \Sigma_k A_{V_k V_k}^{LS}}{\sqrt{3\Sigma_k A_{V_k V_k}^{SS}}} \qquad (58)$$

and

$$\frac{af_\rho^{(1)}}{f_\rho^{(0)}} = -i \sinh am_\rho \frac{\Sigma_k A_{T_{k4} T_{k4}}^{LS} \sqrt{\Sigma_k A_{V_k V_k}^{SS}}}{\Sigma_k A_{V_k V_k}^{LS} \sqrt{\Sigma_k A_{T_{k4} T_{k4}}^{SS}}}. \qquad (59)$$

In Tables XIV and XV we give the lattice results for the matrix elements calculated from the above formulas. The fits to the correlation functions, as for the masses, are all made using the bootstrap method.

Collecting all the terms, the physical decay constants are given by

$$f_\pi = (1 + b_A am) Z_A (f_\pi^{(0)} + c_A af_\pi^{(1)}),$$

$$f_{a_1} = (1 + b_A am) Z_A f_{a_1}^{(0)}, \qquad (60)$$

$$1/f_\rho = (1 + b_V am) Z_V (f_\rho^{(0)} + c_V af_\rho^{(1)}).$$

When the improvement terms are weighted with the appropriate c factors, they contribute about 10–20 % at $\beta = 6.0$ and up to 10% at $\beta = 6.2$. It is thus important to improve the operators as well.

To perform the chiral extrapolation, we make fits similar to those for the hadron masses, namely,

$$f_\pi^2 = b_0 + b_2 m_\pi^2 + b_3 m_\pi^3, \qquad (61)$$

$$f_{a_1}^2 = b_0 + b_2 m_\pi^2 + b_3 m_\pi^3, \qquad (62)$$

$$1/f_\rho^2 = b_0 + b_2 m_\pi^2 + b_3 m_\pi^3. \qquad (63)$$

TABLE XVI. The decay constants f_π, and f_{a_1}, and f_ρ extrapolated to the chiral limit, as well as f_K, f_{K*} taken at the physical quark mass.

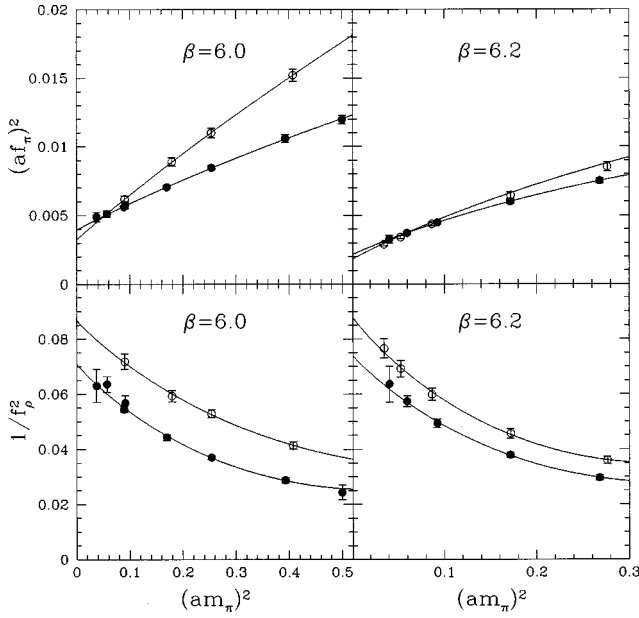| β	c_{SW}	af_π	f_{a_1}	$1/f_\rho$	af_K	$1/f_{K*}$
6.0	0	0.0569(77)	0.2240(76)	0.295(11)	0.0732(26)	0.2385(24)
6.2	0	0.0423(36)	0.2429(48)	0.2971(71)	0.0537(11)	0.2345(28)
6.0	1.769	0.0627(20)	0.195(10)	0.2664(39)	0.0721(8)	0.2020(13)
6.2	1.614	0.0462(38)	0.2130(45)	0.2726(74)	0.0557(14)	0.2149(19)

FIG. 15. Fits and chiral extrapolations of the decay constants f_π and f_ρ for improved (●) and Wilson (○) fermions.

We decided to fit the square of the decay constants rather than the decay constants themselves because this shows less curvature. The fits and the data are shown in Fig. 15 for f_π and f_ρ. We compare this result with the meson decay constants computed with the Wilson action. These follow from Eq. (60) with $c_A, c_V = 0$. For Z_A we use the tadpole-improved value given in Eq. (46), and for b_A we take the tree-level result ($b_A = 1$). The renormalization constant Z_V (in the chiral limit) has been determined nonperturbatively from a two-point correlation function of the local vector current [51] at $\beta = 5.9$, 6.1 and 6.3. Unlike the case of Z_A, we find significant differences between this determination and our determination using the nucleon three-point function. The latter gives $Z_V = 0.651(15)$ at $\beta = 6.0$ which is close to the tadpole-improved result. This indicates large $O(a)$ effects. Since we are applying Z_V to a two-point function, we chose to use the nonperturbative result from Ref. [51]. We interpolate this result to $\beta = 6.0$ and 6.2 and find $Z_V = 0.565$ and 0.618, respectively. For b_V we again take the tree-level result. Although the individual contributions of the improvement terms are significant, the overall result for f_π in Fig. 15 is not much changed when compared with the Wilson case for smaller quark masses. For larger quark masses, especially at $\beta = 6.0$, the Wilson f_π is larger. The situation is different for f_ρ. Here we find a systematic difference of 10–20 % at $\beta = 6.0$ and approximately 10% at $\beta = 6.2$ for all quark masses. In both cases the difference between the two actions becomes smaller with increasing β as one would expect.

Our results extrapolated to the chiral limit are given in Table XVI, and we compare f_π and f_ρ with experiment in Fig. 16. For f_π we find reasonable agreement of the improved results with the experimental value using, as before, the string tension as the scale. When including the data of Ref. [54], one sees that the Wilson results lie lower, and it appears that the values are increasing as we approach the continuum limit. For f_ρ both our improved and Wilson results lie within 5% of the experimental value. There is, how-
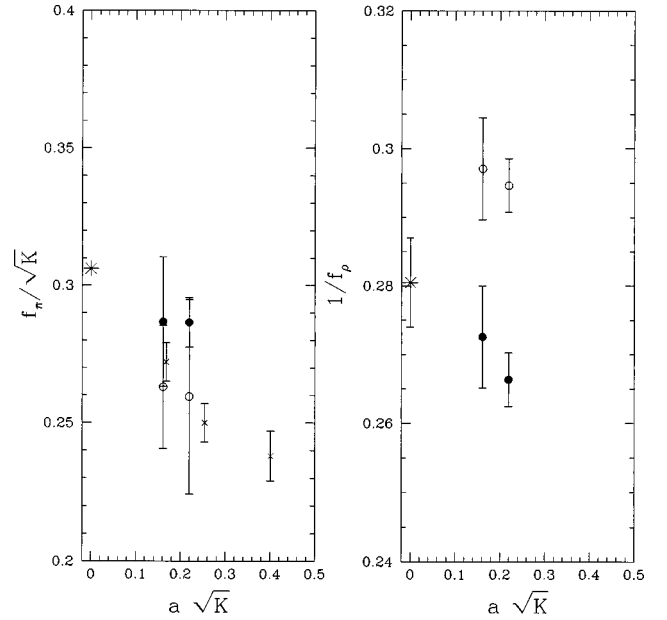

FIG. 16. The decay constants f_π and f_ρ as a function of the lattice spacing for improved (●) and Wilson (○) fermions together with the experimental values (∗). The errors on f_ρ for improved fermions are statistical only. Our results for f_π are compared with the Wilson results of Ref. [54] (×).

ever, a definite difference as we previously remarked. The Wilson numbers lie above the experimental value, while the improved ones lie below. One must remember though that in the Wilson case there is a systematic error in the renormalization constant Z_V which may be larger than the statistical errors in the figure. The experimental number for the decay constant of the a_1 is [55] $f_{a_1} = 0.17(2)$ (in our notation). The
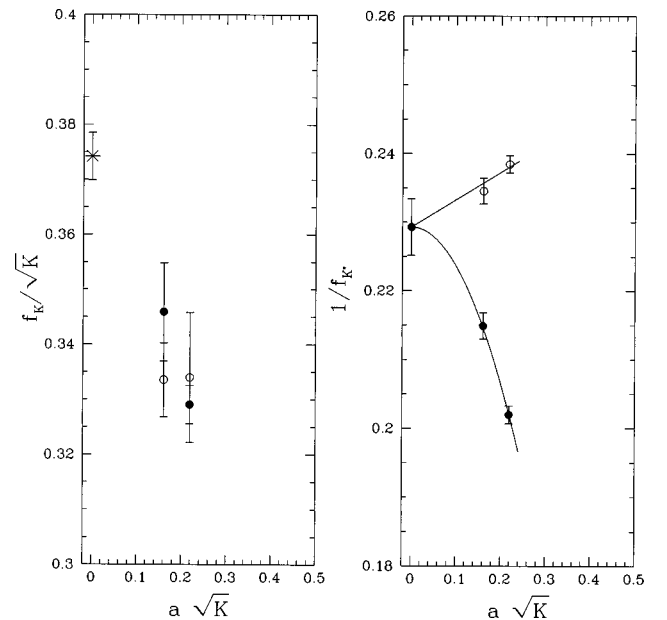

FIG. 17. The decay constants f_K and f_{K*} as a function of the lattice spacing for improved (●) and Wilson (○) fermions. The errors on f_{K*} for improved fermions are statistical only. The solid lines in the f_{K*} figure are from a simultaneous linear fit to the Wilson data and a quadratic fit to the improved data. Our results for f_K are compared with the experimental value (∗).

agreement between experimental and lattice values is encouraging.

We can avoid errors from extrapolating to the chiral limit by considering quark masses within our data range, as we have already done in Figs. 6 and 7. The most physical κ values to use are those corresponding to the K mass. To obtain the decay constants we take Eqs. (61) and (63) at $m_\pi = m_K$. (Remember that we are using m_π as a generic name for the pseudoscalar meson mass.) We give the results for f_K and f_{K*} in Table XVI, and in Fig. 17 we show the scaling behavior together with the experimental value for f_K. We find the errors to be substantially reduced. For f_K we see no difference between improved and Wilson results, both lying 10% below the experimental value. For f_{K*} the error bars have become small enough to attempt an extrapolation to the continuum limit. The curves are a simultaneous fit, linear for the Wilson and quadratic for the improved data, constrained to agree in the continuum limit. In this quantity there appear to be large $O(a^2)$ effects in the improved case.

VI. CONCLUSIONS

The goal of this paper was to investigate the scaling behavior of $O(a)$-improved fermions. If scaling is good, the results we get should already be close to the continuum values for present values of the coupling. To this end we have done simulations for two values of β and looked at two-point correlation functions from which we derive hadron masses, quark masses, and meson decay constants.

First we looked at hadron masses. The most visible difference between Wilson and improved fermions is that the ρ mass is much lighter in the Wilson case at comparable pion masses. In Fig. 6 we see that the improved action has brought the ρ mass closer to its physical value when we use the string tension to set the scale. In this figure we have compared the Wilson action ρ masses at many different scales. We see a linear behavior in the lattice spacing a as one would expect. For improved fermions we find the discretization errors reduced for our couplings.

A problem with Wilson fermions was that they could not describe the vector-pseudoscalar mass splitting adequately. This problem seems to be cured by using improved fermions.

Quark masses are important parameters in the standard model. Experimentally, their values are poorly known, and a reliable lattice determination would be useful. Using two different methods, we have determined the light and strange quark masses. Our results can be seen in Figs. 11 and 12. Both methods give consistent results for improved fermions. In the continuum limit we find for the average of u and d quark masses $m_{u,d}^{\overline{\text{MS}}}(2 \text{ GeV}) = 5.1 \pm 0.2$ MeV and $m_s^{\overline{\text{MS}}}(2 \text{ GeV}) = 112 \pm 5$ MeV. In the Wilson case the discrepancy between the two methods is much larger, hinting at substantial $O(a)$ effects.

When calculating the decay constants, an advantage of using the improved theory is that the renormalization constants and improvement coefficients for f_π, f_{a_1}, f_ρ, and f_{K*} are known. For f_K we still have to use the perturbative values of b_A because they have not yet been computed nonperturbatively. A systematic uncertainty in the Wilson case lies in the choice of the renormalization constants. While the results are in reasonable agreement with phenomenology, the data are at present not precise enough to discuss an extrapolation to the continuum limit, with the possible exception of f_{K*}. In that case it looks that there are relatively large $O(a^2)$ effects between $\beta = 6.0$ and 6.2.

Our general conclusion is that the Wilson action at $\beta = 6.0$ has $O(a)$ errors of up to 20% compared to the continuum extrapolation. The nonperturbatively $O(a)$-improved theory still shows $O(a^2)$ effects of up to 10% at $\beta = 6.0$, except for the Ward identity quark masses where the effect is somewhat larger. If one wants to go to smaller values of β, one probably will have to reduce the $O(a^2)$ errors as well. Going to $\beta = 6.2$ reduces a^2 by a factor of almost 2, bringing discretization errors down to 5% or less. To achieve a one percent accuracy would require calculations at several β values and an extrapolation to $a = 0$.

[1] K. Symanzik, Nucl. Phys. **B226**, 187 (1983); **B226**, 205 (1983).

[2] M. Lüscher and P. Weisz, Commun. Math. Phys. **97**, 59 (1985); **98**, 433(E) (1985).

[3] B. Sheikholeslami and R. Wohlert, Nucl. Phys. **B259**, 572 (1985).

[4] M. Lüscher, S. Sint, R. Sommer, P. Weisz, and U. Wolff, Nucl. Phys. **B491**, 323 (1997).

[5] M. Göckeler, R. Horsley, H. Perlt, P. Rakow, G. Schierholz, A. Schiller, and P. Stephenson, Phys. Lett. B **391**, 388 (1997).

[6] M. Göckeler, R. Horsley, E.-M. Ilgenfritz, H. Perlt, P. Rakow, G. Schierholz, and A. Schiller, in *Lattice '94*, Proceedings of the International Symposium, Bielefeld, Germany, edited by F. Karsch *et al.* [Nucl. Phys. B (Proc. Suppl.) **42**, 337 (1995)].

[7] M. Göckeler, R. Horsley, E.-M. Ilgenfritz, H. Perlt, P. Rakow, G. Schierholz, and A. Schiller, Phys. Rev. D **53**, 2317 (1996).

[8] M. Göckeler, R. Horsley, E.-M. Ilgenfritz, H. Oelrich, H. Perlt, P. Rakow, G. Schierholz, A. Schiller, and P. Stephenson, in *Lattice '96*, Proceedings of the International Symposium, St. Louis, Missouri, edited by C. B. Bernard *et al.* [Nucl. Phys. B (Proc. Suppl.) **53**, 312 (1997)].

[9] H. van der Vorst, SIAM (Soc. Ind. Appl. Math.) J. Sci. Stat. Comput. **12**, 631 (1992).

[10] A. Frommer, V. Hannemann, B. Nockel, T. Lippert, and K. Schilling, Int. J. Mod. Phys. C **5**, 1073 (1994).

[11] C. Best, M. Göckeler, R. Horsley, E.-M. Ilgenfritz, H. Perlt, P. Rakow, A. Schäfer, G. Schierholz, A. Schiller, and S. Schramm, Phys. Rev. D **56**, 2743 (1997).

[12] S. R. Sharpe, in *Lattice '92*, Proceedings of the International Symposium, Amsterdam, The Netherlands, edited by J. Smit and P. van Baal [Nucl. Phys. B (Proc. Suppl.) **30**, 213 (1993)].

[13] D. Weingarten, in *Lattice '93*, Proceedings of the International Symposium, Dallas, Texas, edited by T. Draper *et al.* [Nucl. Phys. B (Proc. Suppl.) **34**, 29 (1994)].

[14] G. P. Lepage and P. B. Mackenzie, Phys. Rev. D **48**, 2250 (1993).

[15] G. S. Bali, Wuppertal Report No. WUB 93-37, 1993, hep-lat/9311009.

[16] Ph. de Forcrand, M. Fujisaki, M. Okuda, T. Hashimoto, S. Hioki, O. Miyamura, A. Nakamura, I. O. Stamatescu, Y. Tago, and T. Takaishi, Nucl. Phys. **B460**, 416 (1996).

[17] P. Bacilieri, E. Remiddi, G. M. Todesco, S. Cabasino, N. Cabibbo, L. A. Fernandez, E. Marinari, P. Paolucci, G. Parisi, G. Salina, A. Tarancon, F. Coppola, M.-P. Lombardo, E. Simeone, R. Tripiccione, G. Fiorentini, A. Lai, F. Marzano, F. Rapuano, and W. Tross, Phys. Lett. B **214**, 115 (1988); M. Guagnelli, M.-P. Lombardo, E. Marinari, G. Parisi, and G. Salina, Nucl. Phys. **B378**, 616 (1992).

[18] C. R. Allton, V. Gimenez, L. Giusti, and F. Rapuano, Nucl. Phys. **B489**, 427 (1997).

[19] S. Collins, in *Lattice '92* [12], p. 393.

[20] F. Butler, H. Chen, J. Sexton, A. Vaccarino, and D. Weingarten, Nucl. Phys. **B430**, 179 (1994).

[21] Y. Iwasaki, K. Kanawa, T. Yoshié, T. Hoshino, T. Shirakawa, Y. Oyanagi, S. Ichii, and T. Kawai, Phys. Rev. D **53**, 6443 (1996); T. Yoshié, Y. Iwasaki, K. Kanaya, S. Sakai, T. Hoshino, T. Shirakawa, and Y. Oyanagi, in *Lattice '91*, Proceedings of the International Symposium, Tsukuba, Japan, edited by M. Fukugita *et al.* [Nucl. Phys. B (Proc. Suppl.) **26**, 281 (1992)].

[22] T. Bhattacharya, R. Gupta, G. Kilcup, and S. Sharpe, Phys. Rev. D **53**, 6486 (1996).

[23] S. Aoki, M. Fukugita, S. Hashimoto, Y. Iwasaki, K. Kanaya, Y. Kuramashi, H. Mino, M. Okawa, A. Ukawa, and T. Yoshié, in *Lattice '95*, Proceedings of the International Symposium, Melbourne, Australia, edited by T. D. Kieu *et al.* [Nucl. Phys. B (Proc. Suppl.) **47**, 354 (1996)].

[24] K. M. Bitar, R. G. Edwards, U. M. Heller, A. D. Kennedy, T. A. DeGrand, S. Gottlieb, A. Krasnitz, J. B. Kogut, W. Liu, P. Rossi, M. C. Ogilvie, R. L. Renken, D. K. Sinclair, R. L. Sugar, D. Toussaint, and K. C. Wang, Phys. Rev. D **46**, 2169 (1992).

[25] M. Fukugita, Y. Kuramashi, M. Okawa, and A. Ukawa, Phys. Rev. Lett. **75**, 2092 (1995).

[26] J. N. Labrenz and S. R. Sharpe, in *Lattice '93* [13], p. 335.

[27] Guagnelli *et al.* [17].

[28] S. Aoki, G. Boyd, R. Burkhalter, S. Hashimoto, N. Ishizuka, in Y. Iwasaki, K. Kanaya, Y. Kuramashi, M. Okawa, A. Ukawa, and T. Yoshié, in *Proceedings of Lattice QCD on Parallel Computers*, Tsukuba, Japan, edited by Y. Iwasaki *et al.* [Nucl. Phys. B (Proc. Suppl.) **60A**, 14 (1998)].

[29] R. Sommer, Nucl. Phys. **B411**, 839 (1994).

[30] H. Wittig, in *Lattice '97*, Proceedings of the International Symposium, Edinburgh, Scotland, edited by C. T. H. Davies *et al.* [Nucl. Phys. B (Proc. Suppl.) **63**, 47 (1998)].

[31] R. Sommer, Phys. Rep. **275**, 1 (1996).

[32] G. S. Bali and K. Schilling, Phys. Rev. D **47**, 661 (1993).

[33] S. P. Booth, D. S. Henty, A. Hulsebos, A. C. Irving, C. Michael, and P. W. Stephenson, Phys. Lett. B **294**, 385 (1992).

[34] H. Wittig, in *Lattice '94* [6], p. 288.

[35] H. Hoeber (private communication); Ref. [32] reanalyzed with link integration.

[36] C. R. Allton, C. T. Sachrajda, R. M. Baxter, S. P. Booth, K. C. Bowler, S. Collins, D. S. Henty, R. D. Kenway, C. McNeile, B. J. Pendleton, D. G. Richards, J. N. Simone, A. D. Simpson, A. McKerrell, C. Michael, and M. Prisznyak, Nucl. Phys. **B407**, 331 (1993).

[37] S. Perantonis and C. Michael, Nucl. Phys. **B347**, 854 (1990).

[38] K. D. Born, R. Altmeyer, W. Ibes, E. Laermann, R. Sommer, T. F. Walsh, and P. M. Zerwas, in *Lattice '90*, Proceedings of the International Symposium, Tallahassee, Florida, edited by U. M. Heller *et al.* [Nucl. Phys. B (Proc. Suppl.) **20**, 394 (1991)].

[39] E. Eichten, K. Gottfried, T. Kinoshita, K. D. Lane, and T. M. Yan, Phys. Rev. D **21**, 203 (1980).

[40] M. Campostrini and C. Rebbi, Phys. Lett. B **193**, 78 (1987).

[41] For a review see, for example, M. Neubert, CERN Report No. CERN-TH/96-292, 1996, hep-ph/9610266.

[42] H. Pagels, Phys. Rev. D **19**, 3080 (1979).

[43] Particle Data Group, R. M. Barnett *et al.*, Phys. Rev. D **54**, 1 (1996).

[44] M. Lüscher, S. Sint, R. Sommer, and P. Weisz, Nucl. Phys. **B478**, 365 (1996).

[45] M. Lüscher, S. Sint, R. Sommer, and H. Wittig, Nucl. Phys. **B491**, 344 (1997).

[46] S. Sint and P. Weisz, Nucl. Phys. **B502**, 251 (1997).

[47] S. Capitani, M. Göckeler, R. Horsley, H. Perlt, P. Rakow, G. Schierholz, and A. Schiller, in *Lattice '97* [30], p. 874.

[48] M. Göckeler, R. Horsley, H. Oelrich, H. Perlt, P. Rakow, G. Schierholz, and A. Schiller (in preparation).

[49] H. Leutwyler, Phys. Lett. B **378**, 313 (1996).

[50] M. Göckeler, R. Horsley, H. Oelrich, H. Perlt, P. Rakow, G. Schierholz, and A. Schiller, in *Lattice '95* [23], p. 493.

[51] S. Aoki, M. Fukugita, S. Hashimoto, N. Ishizuka, Y. Iwasaki, K. Kanaya, Y. Kuramashi, H. Mino, M. Okawa, A. Ukawa, and T. Yoshié, in *Lattice '96* [8], p. 209.

[52] R. Gupta and T. Bhattacharya, Phys. Rev. D **55**, 7203 (1997).

[53] R. Sommer, in *Lattice QCD on Parallel Computers* [28], p. 279.

[54] F. Butler, H. Chen, J. Sexton, A. Vaccarino, and D. Weingarten, Nucl. Phys. **B421**, 217 (1994).

[55] M. Wingate, T. DeGrand, S. Collins, and U. M. Heller, Phys. Rev. Lett. **74**, 4596 (1995).